MATERIALS CHEMISTRY FRONTIERS

REVIEW

View Article Online
View Journal | View Issue

Cite this: *Mater. Chem. Front.*, 2023, **7**, 5786

Recent progress of two-dimensional Ruddlesden–Popper perovskites in solar cells

Chao Wang,[a] Xinhe Dong,[a] Feifan Chen,[a] Guozhen Liu *[b] and Haiying Zheng *[a]

Received 12th May 2023,
Accepted 6th August 2023

DOI: 10.1039/d3qm00547j

rsc.li/frontiers-materials

Two-dimensional (2D) perovskites, as an important part of organic–inorganic hybrid halide perovskite materials, have attracted increasing attention owing to their excellent stability, especially water resistance, and become a research hotspot in the field of perovskite solar cells (PSCs). This review mainly summarizes the application of 2D Ruddlesden–Popper (RP) perovskite materials based on different spacer cations in solar cells. First, we briefly introduce the structure and classification of 2D perovskite materials. Then, the research progress of 2D RP perovskite materials based on several typical spacer cations is discussed, mainly including the performance improvement strategy, surface passivation application, and mechanism research. Finally, we also briefly prospect the present challenges and future development direction of 2D RP PSCs.

1. Introduction

In recent years, owing to the advantages, such as strong light capture ability, low trap state, excellent carrier transport, long charge carrier mobility,[1] great ability to tolerate defects,[2] fast mobility,[3] very narrow photoluminescence, high quantum yield,[4] efficient photoexciton dissociation, and easy solution preparation process, perovskite solar cells (PSCs) have attracted considerable interest and thus are being fully studied. The power conversion efficiency (PCE) of PSCs has shown a significant increase from 3.8% to 26.0%[5,6] making them a viable alternative to traditional silicon-based solar cells. However, perovskite materials have exhibited relatively poor stability under humidity, light, and high temperature, which have seriously hindered their large-scale commercial applications.[7] Therefore, it has emerged as a prominent research area to enhance the stability of PSCs with a focus on developing effective strategies, including two-dimensional (2D) perovskites,[8–13] all-inorganic perovskites,[14–16] component engineering,[17–19] defect passivation engineering,[20–22] interface modification engineering,[23–25] encapsulation technology,[26] and device structure engineering.[27,28]

Among them, 2D perovskite materials (in this review, the 2D perovskite materials are the unified name for layered perovskites, including pure 2D perovskites, layered hybrid perovskites, 2D homologous perovskites, 2D perovskites, quasi-2D perovskites, 2D-3D perovskites, low-dimensional (LD) perovskites, and mixed-dimensional (MD) perovskites) replacing 3D

[a] *Institutes of Physical Science and Information Technology, Anhui University, Hefei 230601, P. R. China. E-mail: hyzheng@ahu.edu.cn*
[b] *State Key Laboratory of Fine Chemicals, School of Chemistry, Dalian University of Technology, Dalian 116024, China*

Chao Wang

Chao Wang received his bachelor's degree from West Anhui University in 2022. Currently, he is a master's student under the supervision of Dr Haiying Zheng in the Institutes of Physical Science and Information Technology, Anhui University. His current research focuses on the development of stable and efficient mixed-dimensional perovskite solar cells.

Xinhe Dong

Xinhe Dong has graduated with a bachelor's degree from the North University of China in 2021. She is currently studying for her master's degree under the guidance of Dr Haiying Zheng in the Institutes of Physical Science and Information Technology, Anhui University. Her current research interest includes the preparation of highly efficient and stable 2D/3D perovskite solar cells.

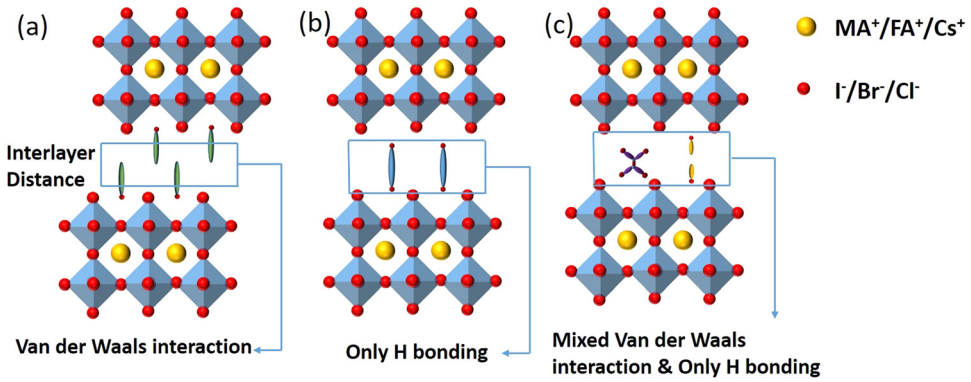

Fig. 1 Crystal structures of the three 2D perovskites. (a) RP phase, (b) DJ phase, and (c) ACI phase.

perovskites as the light absorption layers is the most fundamental and effective way to improve the stability of PSCs from the material itself, but the PCEs of 2D perovskite devices have not been ideal. The low PCEs are mainly caused because the organic spacer cations with large-sized aromatic or aliphatic groups although can improve the self-assembly capacity and inherent chemical stability of the 2D perovskite materials, it makes the 2D perovskites exhibit stronger quantum and dielectric constraints, resulting in higher band gap (E_g) and larger exciton binding energy.[29–32] Therefore, it is necessary to distinguish the impact of various organic spacer cations on the properties of the resulting 2D perovskites to identify and design suitable organic spacers that can enhance the PCE of 2D perovskite devices.

In this review, we first introduce the structure and classification of 2D perovskite materials and then mainly focus on the research progress, performance improvement strategies, surface passivation application, and limitations of these 2D Ruddlesden–Popper (RP) perovskite materials started from several typical spacer cations, such as long chain organic ammonium salts represented by butylammonium (BA), phenyl organic ammonium salts represented by phenylethylammonium (PEA), organic ammonium salts with halogen groups and organic ammonium salts with heterocycle groups. The challenges are summarized and the future research direction is prospected for 2D RP perovskite materials.

2. Structure and properties of 2D perovskite materials

2D perovskites are generally obtained from their corresponding organic–inorganic halide 3D perovskites (ABX_3) by appropriately increasing the distance between the interconnected inorganic sheets and the organic cations along the direction of ⟨100⟩. The 2D perovskite compounds can be expressed using the general

Feifan Chen

Feifan Chen received his bachelor's degree from Liaocheng University in 2022. He is now pursuing master's degree in material chemical engineering under the supervision of Dr Haiying Zheng in the Institutes of Physical Science and Information Technology, Anhui University. His current research focuses on the development of stable and efficient perovskite solar cells with a research direction of electrochemistry.

Guozhen Liu

Guozhen Liu received his PhD in materials physics and chemistry from the University of Science and Technology of China in 2020. He is currently working as a Postdoc fellow under the guidance of Prof. Yantao Shi in the State Key Laboratory of Fine Chemicals, School of Chemistry, Dalian University of Technology. His current research focuses on the large-area and flexible perovskite solar cells.

Haiying Zheng

Haiying Zheng is a research associate in the Institutes of Physical Science and Information Technology, Anhui University. She received her PhD in materials physics and chemistry from the University of Science and Technology of China in 2019. Now her present interests are focused on new-type solar cells, especially two dimensional and mixed-dimensional perovskite solar cells.

formula $A/A_2A'_{n-1}B_nX_{3n+1}$, where A and A′ denote organic cations, B denotes divalent metal cations (Pb^{2+}, Sn^{2+} or Ge^{2+}), and X represents halide ions. According to different crystal structural characteristics, 2D perovskites can be categorized into three types, including the RP phase, Dion–Jacobson (DJ) phase, and alternating cations in the interlayer space (ACI). Fig. 1 shows the crystal structures of the three 2D perovskites.

The 2D layered perovskites with the RP phase structure are the predominant type and have many important applications. The general formula of the RP phase 2D perovskites is $A'_2A_{n-1}B_nX_{3n+1}$, and the structure is shown in Fig. 1a, where A′ is an organic spacer cation (*e.g.* PEA^+, BA^+), A is methylamine (MA^+) or formamidine (FA^+), B represents metal ions (*e.g.* Pb^{2+} or Sn^{2+}), X represents halogen ions, n is the number of octahedra between spacer layers, which greatly affects the photoelectric properties of RP perovskites. When $n = 1$, the organic cation separates single inorganic $[BX_6]^{4-}$ flakes to form the pure 2D A'_2BX_4 perovskite. When $n > 1$, organic cations are introduced into the multilayer structure, and 2D RP structures are formed. When $n = \infty$, it corresponds to the 3D cubic structure of ABX_3.[31] In early studies for 2D RP perovskites, the PCEs of 2D RP PSCs were universally low due to the insulation of spacer cations. As the research went on, it was found that the hot casting technology was used to prepare vertically oriented 2D RP films to overcome this obstacle.[33] Later, the PCE could be further improved by inducing the out-of-plane arrangement of the inorganic thin plates. To achieve the out-of-plane arrangement of inorganic thin plates, the additives (such as MACl, NH_4SCN, and NH_4Cl) and the element doping methods were tried.[34–38]

DJ phase 2D perovskites are formed by combining heavy organic diammonium cations into an inorganic framework composed of symmetrical layered arrays. The structure is shown in Fig. 1b. The general formula is $A'A_{n-1}B_nX_{3n+1}$, where A′ is the organic diamine cation. The unique structural characteristics of DJ 2D perovskites are mainly determined by spacer cations.[39] Unlike the RP phase, the DJ phase contains a single divalent interlayer cation between the 3D perovskite inorganic plates, and the divalent cation is vertically combined with the 2D perovskite plates, there is no displacement between the octahedral plates, thus forming a well-arranged layered structure. Meanwhile, it has been found that the van der Waals gap between 2D perovskites can be eliminated by DJ phase 2D perovskites. Subsequently, more 2D DJ perovskites and devices based on various organic diammonium cations have been reported. For example, Li *et al.* proposed a new organic spacer (1, 4-phenyldimethyl ammonium ($PDMA^{2+}$)) to prepare dual-function 2D DJ PSCs, which significantly improved the device efficiency and environmental stability.[40] Liu *et al.* designed a novel (D-A-D (D: donor, A: recipient) type) organic cationic DPP-2T as a 2D spacer, and synthesized $(DPP\text{-}2T)_{0.5}(MA)_{n-1}Pb_nI_{3n+1}$ 2D DJ perovskites, showing effectively the reduced E_g, inhibited charge transfer barrier, extended carrier diffusion length, and improved device performances.[41] Shao *et al.* summarized the research progress of 2D DJ perovskite materials, including their basic structures, optoelectronic and photophysical properties, as well as the strategies used to improve the performances of corresponding 2D DJ PSCs from the perspective of molecular structure design and processing engineering.[42]

The general formula for ACI phase 2D perovskites is $A'A_nM_nX_{3n+1}$, where the slightly larger A′ cation, such as guanidinium (GA^+), and the smaller A-site cations (MA^+/FA^+) alternate in layers to form the structure as shown in Fig. 1c. The new organic cation arrangement of A′ shortens the interlayer distance and eliminates or reduces van der Waals gaps. The ACI phase induces octahedral rotation in the final layered crystal structure by adopting alternated cation arrangements at interlayer positions, resulting in a shorter interlayer distance, compared to the RP phase.[43] Most importantly, ACI phase PSCs have the potential for high light absorption performance and relatively high PCE, thus attracting much attention. For example, Zhang *et al.* have made great achievements in exploring the dynamic changes, optoelectronic properties, morphological manipulation, and the influence of the final photovoltaic performance during the formation of ACI phase perovskite films.[44] Gong *et al.* discussed the advantages and prospects of ACI phase PSCs from a chemical perspective, systematically expounding the potential and the problems to be overcome for ACI phase perovskites.[45] Lu *et al.* clarified the mechanism of spacer cations by comparing the E_g modulation range of the ACI phase and RP phase perovskites, and proposed a method to adjust the E_g of 2D perovskites by selecting different spacer cations.[46]

Due to the unique layered structure of 2D perovskites, they display another attractive property, namely the tunable optical properties. The optical properties of 2D perovskites mainly depend on the thickness and composition of the inorganic layers, and the E_g and exciton binding energy can be greatly regulated by tailoring the n value (the number of inorganic layers between the organic spacer layers). The optical properties of 2D perovskites are gradually close to those of 3D perovskites because the quantum and dielectric confinement effects weaken with the increase of the n value. In addition, the effect of organic spacer cations on the optical properties of 2D perovskites cannot be ignored. On the one hand, the organic layers act as the energy barrier of the inorganic layers, incorporating different organic spacer cations will change the exciton binding energy because of their different dielectric constants. On the other hand, the chain length of the organic spacer cations has a great influence on the distance between adjacent inorganic layers. Furthermore, the organic spacer cations can interact with the inorganic layers through coordination bonds and hydrogen bonds, which can cause the deformation of the inorganic frameworks.[47,48] Therefore, their optical properties can be greatly adjusted by various strategies, such as controlling the thickness and composition of inorganic layers and adjusting the range of organic spacer cations, and new-type efficient and stable 2D PSCs can be designed.

RP phase 2D perovskites have garnered significant attention as one of the pioneering and extensively explored types of 2D perovskite materials, which is mainly caused by their versatility

in incorporating a wide range of organic spacer cations and their impressive optical properties arising from robust quantum and dielectric confinement effects. The unique structural characteristics of RP phase 2D perovskites enable them to display extensive applications and functionalities with tremendous exploration possibilities and research value. Therefore, the performances of 2D RP perovskites can be changed by varying the type and size of organic spacer cations. In this paper, 2D RP perovskite materials based on different spacer cations and their properties are reviewed.

3. 2D RP perovskite materials based on different spacer cations

Since the structure and properties of organic spacer cations have a great impact on the performances of 2D RP perovskites, more and more attention has been paid to the selection of different organic spacer cations to further improve the PCEs of 2D RP PSCs. Hence, in just a few years, many different types of organic spacer cations have emerged, such as butylamine (BA),[49] phenylethylamine (PEA),[50] cyclohexylmethylammonium iodide (CHMA),[51] and tetrapropylammonium (TPA).[52] Next, we will introduce the research progress, limitations, and performance improvement strategies of 2D RP perovskite materials based on different spacer cations.

3.1. The 2D RP perovskites and devices based on the long-chain organic spacer cations represented by BA

As one of the earliest spacer cations, 2D perovskite based on BA was reported as early as 2015. Cao *et al.* prepared $(BA)_{n-1}Pb_nI_{3n+1}$ (n = 1, 2, 3, and 4) perovskite films, and proposed 2D homologous perovskites for the first time. The properties of 2D perovskites with different n values were analyzed in detail and a PCE of 4.02% was obtained.[53] Subsequently, more and more studies have been reported on the long-chain organic spacer cations represented by BA (*e.g.* *n*-hexylammonium (HA),[54] ethylammonium (EA),[55] propylammonium (PA),[56] octylammonium iodide (OA),[57] which greatly promoted the development of 2D PR PSCs.

Compared with 3D PSCs, the PCEs of 2D PSCs are very poor. To improve the photovoltaic performances of 2D RP PSCs based on the long-chain organic spacer cations represented by BA, various methods have been developed, such as component regulation, additive engineering, and ion doping. Component engineering can help expand the research range of materials and regulate their properties, which is an important method to improve the PCEs of 2D RP PSCs. Yan *et al.* used FA^+ as the A-site cation to prepare $(BA)_2(FA)_{n-1}Pb_nI_{3n+1}$ 2D perovskites and it can effectively reduce the E_g of 2D perovskites and make the films have better phase and environmental stability by replacing MA^+ with FA^+ under the same n value (Fig. 2a).[58] Zhang *et al.* introduced Cs^+ into $(BA)_2(MA)_3Pb_4I_{13}$ 2D perovskite to

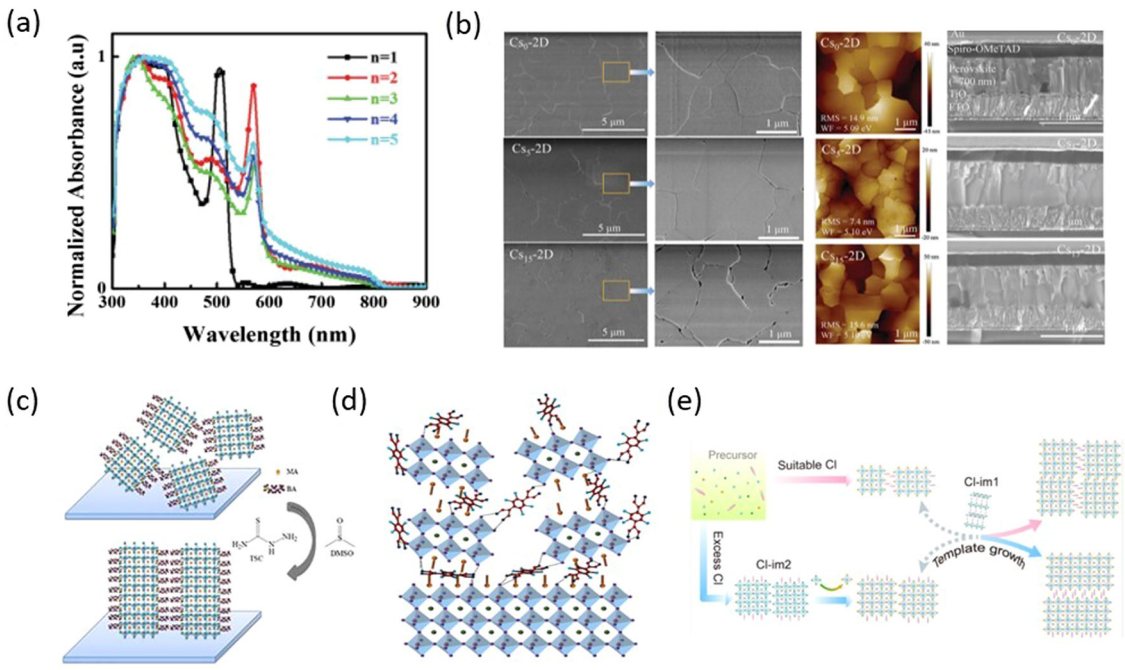

Fig. 2 (a) Normalized absorption spectra of the perovskite $(BA)_2(FA)_{n-1}Pb_nI_{3n+1}$ films with different n values after thermal annealing. Adapted from ref. 58 with permission. Copyright 2018, Royal Society of Chemistry. (b) Morphology characterization of the Cs_x-2D perovskite films. Adapted from ref. 59 with permission. Copyright 2017, Royal Society of Chemistry. (c) Schematic for the random (without additive) and vertical (with additive) orientation relative to the substrate. Adapted from ref. 62 with permission. Copyright 2020, Elsevier. (d) The interfacial structure of PSCs with 3D/2D perovskite films 5% w/w F4TCNQ. Adapted from ref. 63 with permission. Copyright 2020, American Chemical Society. (e) Schematic illustration of the crystal orientation modulation mechanisms for different Cl concentrations. Adapted from ref. 64 with permission. Copyright 2022, American Chemical Society.

partially replace MA^+, due to the improved grain sizes and surface quality (Fig. 2b), the PCE of the device with high environmental stability was increased from 12.3% to 13.7%.[59] Han *et al.* added a suitable amount of $PbBr_2$ into the precursor solution and the result demonstrated that Br^- can improve the morphology and crystallinity of 2D perovskite films, thereby obtaining excellent film quality and high photoelectric performance, significantly increasing PCE from 3.01% to 12.19% (Fig. 2c). In addition, Br^- doping enhances the tolerance of PSCs to humidity, light, and thermal stability.[60] Adding additives in the precursor solution to improve crystallinity and regulate the preferred orientation growth of 2D perovskite crystals is also an effective method to improve PCE. By adding NH_4SCN, Zhang *et al.* prepared the vertically oriented 2D $(BA)_2(MA)_{n-1}Pb_nI_{3n+1}$ PSCs with PCE of 6.82% for n = 3 and 8.79% for n = 4 (Fig. 2d).[61] Zheng *et al.* added both DMSO and thiourea (TSC) into 2D $(BA)_2(MA)_3Pb_4I_{13}$ at the same time. The synergistic effect of DMSO and TSC effectively regulated the crystallization process of 2D perovskite to improve the morphology quality, increase grain sizes and crystallinity, leading to the increased PCE from 1.05% to 14.15% with improved stability (Fig. 2e).[62] Sun *et al.* used 2,3,5,6-tetrafluoro-7,7,8,8-tetracyanoquinodimethane (F4TCNQ) as a molecular additive to be added to the BA-based 2D perovskite layer to alleviate the charge transfer limitation of the 2D perovskite layer in hybrid 3D/2D PSCs. The surface state was effectively passivated by supramolecular interaction between F4TCNQ and halide ions (Fig. 2f). Importantly, the hybrid 3D/2D PSCs displayed higher performances with an improved PCE from 18.1% to over 20% and better humidity stability.[63] By using *in situ* scanning incidence X-ray diffraction technology based on synchrotron radiation, Chen *et al.* studied the crystallization kinetics and chemical transformation pathways of Cl^- additives during the film-forming process of $BA_2MA_3Pb_4I_{13}$ and revealed the regulation mechanism of Cl^-, which can effectively adjust the crystal orientation of 2D perovskite films by forming intermediates (Fig. 2g).[64]

The surface defects of perovskite as charge carrier traps are the key factors limiting the performances of PSCs. Therefore, defect passivation is also a very important method to promote the performances of PSCs, especially the high-stable 2D perovskites as surface modification layers, which become another research direction for 2D RP perovskites. Among them, the 2D RP perovskite passivation layers based on the long-chain organic spacer cations, such as BA, have been most studied. For example, Catchpole *et al.* studied the passivation effects of long-chain organic cations, BABr, and dodecylammonium bromide (DABr), on perovskite. The study showed that the passivation ability of long-chain organic cations is stronger than that of short-chain organic cations, which is conducive to the extraction of holes in the device. The devices with a long alkyl chain passivation layer exhibited increased PCE of 19.1% and significantly improved water and light stability (Fig. 3a).[65] Chen *et al.* mixed perovskite precursors with large-sized organic cations, including BA, EA, DMA, and GA, to spontaneously form the 2D passivation layer at the buried interface. The results indicated that the strong binding between cations and substrates induced preferential crystallization of the 2D perovskite phase, which can act as a passivation layer, resulting in the obtained PSCs with a higher open-circuit voltage (V_{oc}) and a PCE of 22.9% (Fig. 3b).[66] Yang *et al.* reported a simple DGPF self-passivation strategy coating BABr on a 3D perovskite film to simultaneously passivate the internal bulk defects and gradient 2D perovskite interface defects by thermally driving. As a result, the devices showed reduced V_{oc} losses, significantly improved PCE by 23.78%, and greatly enhanced operational stability (Fig. 3c).[67] At present, more and more studies have been conducted to improve the performance of PSCs by introducing

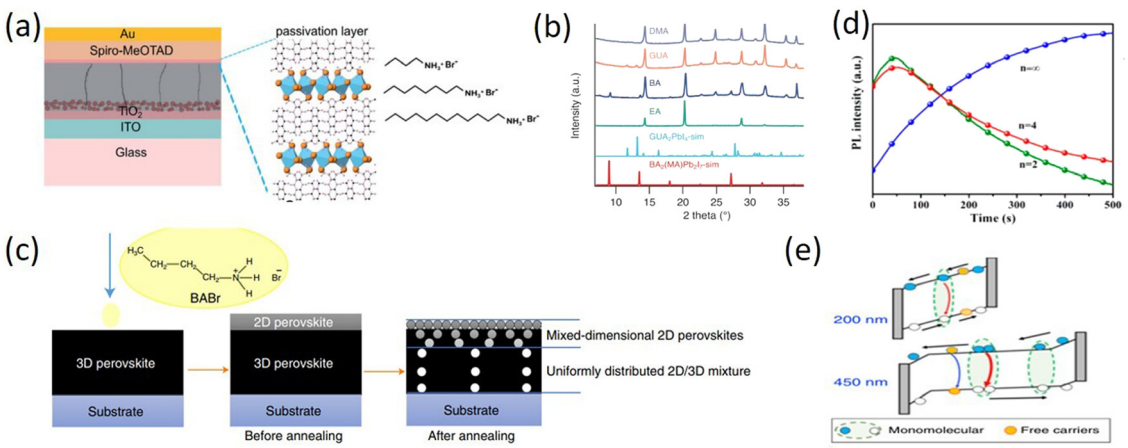

Fig. 3 (a) Schematic of alkylammonium bromide surface passivated perovskite solar cells. Adapted from ref. 65 with permission. Copyright 2021, Royal Society of Chemistry. (b) XRD patterns of DMA-, GUA-, BA-, EA-containing films. Adapted from ref. 66 with permission. Copyright 2021, Wiley. (c) Schematic diagram of the DGPF approach. Adapted from ref. 67 with permission. Copyright 2021, Springer Nature. (d) *In situ* PL measurement for $BA_2(MA)_3Pb_4I1_3$ film by detecting the emission peak at 585 nm (n = 2), 670 nm (n = 4), and 780 (n = ∞). Adapted from ref. 70 with permission. Copyright 2018, American Chemical Society. (e) Schematics illustrating the carrier recombination processes in thin film and thick film in the quantum well-layered perovskite structure. Adapted from ref. 71 with permission. Copyright 2018, Springer Nature.

2D perovskites as the surface modification layers of 3D perovskite. Hence, 2D/3D perovskite heterostructures have been developed and the 2D perovskite-based van der Waals heterostructures have been gradually discovered by integrating 2D perovskite with other layered materials, which provides a new development direction for optoelectronic devices. Wang *et al.* gave a comprehensive description of various heterogeneous structures based on 2D perovskites and proposed their potential research directions. The study of 2D perovskite-based van der Waals heterostructures provides a new revelation for the exploration of 2D RP PSCs, which will further promote the development of PSCs.[68,69]

Nowadays, scientific researchers are not only focusing on finding simple ways to improve the PCE of 2D RP perovskites but also paying more and more attention to the mechanism study. By understanding the internal mechanism process, the internal carrier behavior can be better controlled to improve the PCEs of 2D RP PSCs. For example, Zhuo *et al.* prepared a series of $(BA)_2(MA, FA)_3Pb_4I_{13}$ Q-2D perovskite films to understand the crystallization kinetics of crystal orientation and carrier behavior in polycrystalline films. The research implied that by gradually replacing MA^+ with FA^+, the crystallization kinetics can be effectively controlled to reduce the non-radiative recombination centers, thus obtaining high-quality films (Fig. 3d).[70] Tisa *et al.* used layered 2D $BA_2MA_3Pb_4I_{13}$ PSCs to study the characteristics of PSCs in a planar p–i–n device structure. Through extensive device characterization and modeling, they elucidated the main charge transport mechanism during the operation of PSCs and identified the key bottleneck that limits the overall PCEs of layered 2D PSCs, which is caused by the recombination losses of carriers on potential barriers in vertically stacked layered perovskite quantum well (Fig. 3e).[71] These findings have significant implications for the further development of 2D PSCs.

The performance of 2D RP PSCs with low *n* values based on the long-chain organic spacer cations represented by BA are summarized in Table 1.[53,56–64] Although the 2D RP perovskites based on the long-chain organic spacer cations represented by BA have been greatly developed, it is still the focus of research on these 2D RP PSCs with low *n* values to maintain high stability while having the satisfactory PCE comparable to 3D perovskite, and further mechanism research is also very necessary.

3.2. 2D RP perovskites and devices based on the phenyl organic spacer cations represented by PEA

Smith *et al.* firstly reported the $(PEA)_2(MA)_2Pb_3I_{10}$ layered perovskite material in 2014, which achieved a V_{oc} of 1.18V and a PCE of 4.73%. Although the PCE is not as high as that of 3D perovskite, high-quality films with good moisture resistance can be obtained without annealing by one-step spin coating under environmental conditions.[72] This was the first appearance of layered perovskite materials. Subsequently, together with the BA 2D RP perovskite in 2015, PEA 2D RP perovskite and devices have been rapidly developed. In contrast to the long chain organic spacer cations with poor hydrophobicity and relatively simple structure, the 2D RP perovskite materials based on the phenyl organic spacer cations represented by larger PEA (*e.g.* phenylbutylammonium (PBA),[73] phenylmethylammonium (PMA),[74] phenyltrimethylammonium (PTMA)[75] and benzamidine (PhFA)[76]) have attracted more and more attention, but the performances of the devices are still not satisfactory. Many strategies have been proposed to improve the PCEs of PEA 2D PSCs.

In view of the flexible replaceable characteristics of perovskite materials, scientists proposed that component engineering should involve a variety of substitution or partial substitution doping to adjust the E_g, enhance structural stability, and ultimately improve device performances. Since Smith *et al.* first proposed and prepared 2D PSCs with PEA as spacer cations, many scientists have been studying how to regulate the components to improve the PCE of phenyl-based 2D RP perovskite devices. Cui *et al.* added Rb^+ into the precursor solution and found that the added Rb^+ preferentially accumulated in the crystal growth front to form the Rb^+-enriched regions that suppressed the absorption and diffusion of organic cations at the growth front, thereby regulating the crystal growth rate (Fig. 4a). The delayed crystal growth is favorable for improving the crystal quality and carrier recombination lifetime of PEA 2D perovskite films, which can significantly improve the PCE from 12.5% to 14.6%.[77] Yu *et al.* prepared the $(BDA)_{1-a}(PEA_2)_a$-$MA_4Pb_5X_{16}$ 2D perovskite with two different spacer cations, 1,4-butanediammonium (BDA) and PEA. By simply mixing the BDA and PEA, the $(BDA)_{0.8}(PEA_2)_{0.2}MA_4Pb_5X_{16}$ self-assembled polycrystalline film was obtained with smaller exciton binding energy, uniformly distributed quantum wells and better carrier transport, leading to an optimized PCE of 17.21% and

Table 1 Performance summary of 2D RP PSCs (low *n* value) based on the long chain organic spacer cations represented by BA

Spacer	Strategy	Component	Stability	PCE (%)	Ref.
BA	—	$(BA)_2(MA)_{n-1}Pb_nI_{3n+1}$	High humidity, maintain PCE for a long time	4.02	53
	FA^+ as A-site	$(BA)_2(FA)_{n-1}Pb_nI_{3n+1}$	80% of initial PCE under RH (25 ± 5%) for 25 d	6.88	58
	Cs^+ doping	$(BA)_2(MA)_3Pb_4I_{13}$	RH 30%, 90% of initial PCE for 1400 h	13.7	59
	Br^- doping	$BA_2MA_4Pb_5I_{16-10x}Br_{10x}$	Unsealed, good stability	12.19	60
	NH_4SCN additive	$(BA)_2(MA)_{n-1}Pb_nI_{3n+1}$	Unsealed, PCE unchanged in a pure N_2 glove box	8.79	61
	DMSO & TSC	$(BA)_2(MA)_3Pb_4I_{13}$	RH (25 ± 5%), air for 720 h 90.3% of initial PCE	14.15	62
	F4TCNQ additive	$BA_2(FA)_{n-1}Pbn(I/Br)_{3n+1}$	80% of initial PCE under ~60% RH for 30 d	20	63
	Cl^- doping	$BA_2MA_3Pb_4I_{13}$	RH (34–40%) for 15 d, no degradation		64
PA		$(PA)_2(MA)_{n-1}Pb_nI_{3n+1}$	RH (20–80%) ± 5% for 450 d		56
OA	—	$(OA)_2(FA)_{n-1}Sn_nI_{3n+1}$	Unsealed, N_2, 80% of initial PCE for 14 d	3.03	57

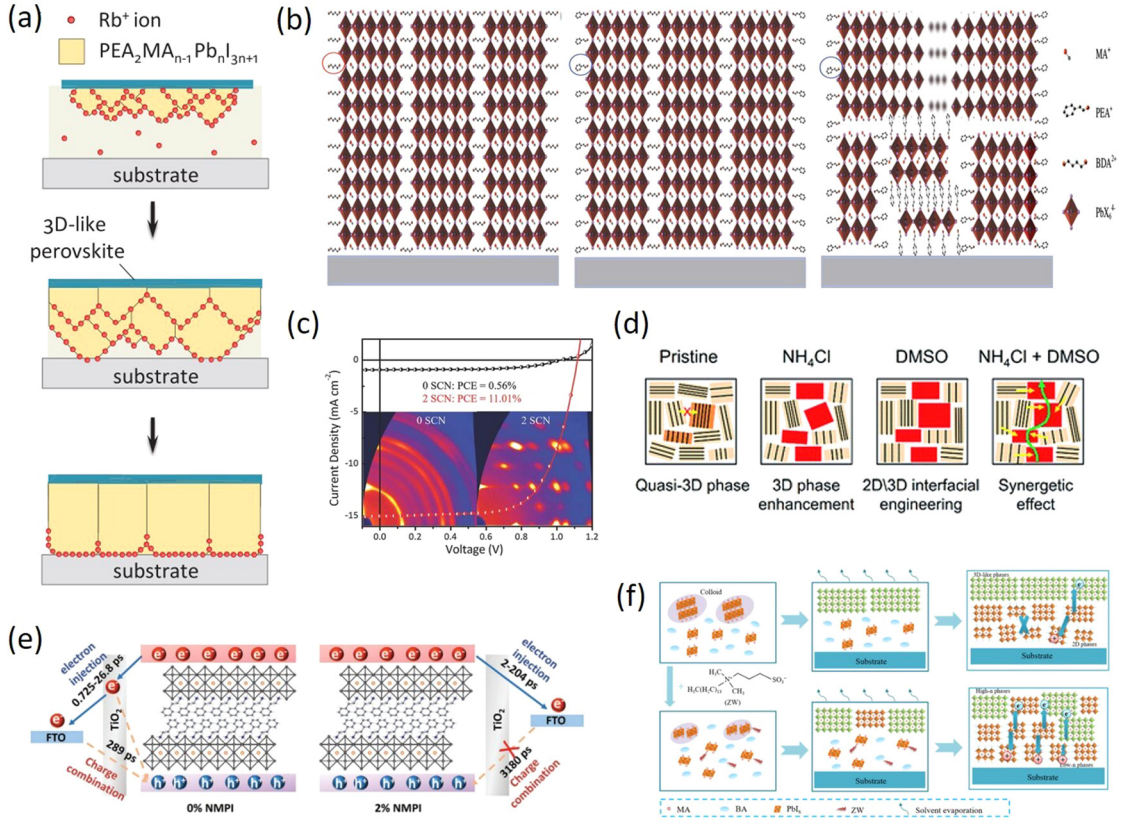

Fig. 4 (a) Illustration of the dynamic distribution of Rb^+ ions during the crystallization process. Adapted from ref. 77 with permission. Copyright 2020, Wiley. (b) Schematic illustration of the perovskite film structure for BDA, $(BDA)_{0.8}(PEA_2)_{0.2}$ and PEA_2 films. Adapted from ref. 78 with permission. Copyright 2021, Wiley. (c) 2D GIWAXS patterns and *J*–*V* curves of $(PEA)_2(MA)_4Pb_5I_{16}$ (n = 5) perovskite with and without NH_4SCN. Adapted from ref. 35 with permission. Copyright 2018, Wiley. (d) Schematic crystal structure of PEA, PEA + NH_4Cl, PEA + DMSO, and PEA + NH_4Cl + DMSO based 2D perovskites. Adapted from ref. 81 with permission. Copyright 2019, Royal Society of Chemistry. (e) Carrier behaviors of quasi-2D (n = 20) $CsPbI_3$ films. Adapted from ref. 82 with permission. Copyright 2021, Wiley. (f) Schematic representation indicating the crystallization process for both control (top) and ZW-treated (bottom) 2D RPLP films. Adapted from ref. 83 with permission. Copyright 2022, American Chemical Society.

complementary humidity and thermal stability for PSCs (Fig. 4b).[78] Ramos *et al.* heavily doped Gua^+ into 2D RP perovskites and explored the binding of Gua^+ with the octahedral position of the "perovskite sheet" for the first time. The mixed-cation $PEA_2(MA_{1-x}Gua_x)_2Pb_3I_{10}$ perovskite films were synthesized by gradually replacing MA^+ with Gua^+ and the addition of Gua^+ controlled the optoelectronic properties of 2D RP PSCs, which proved the positive effect on the degradation of 2D RP perovskites.[79]

The addition of small organic molecules can not only improve the PCEs of BA 2D RP PSCs but also enhance the PCEs of phenyl-based 2D perovskite devices, thus additive engineering has been widely studied in these 2D PSCs. Yan *et al.* reported that adding methylammonium acetate (MAAc) as an additive in the precursor solution can improve the performances of 2D $(PEA)_2(MA)_2Pb_3I_{10}$ prepared by a one-step solution method. Under suitable MAAc molar ratios, the 2D perovskite films exhibited improved surface smoothness, increased coverage, and higher crystalline quality, which ultimately resulted in the elimination of *J*–*V* hysteresis.[80] Zhang *et al.* attempted to use NH_4SCN as an additive to prepare $(PEA)_2(MA)_{n-1}Pb_nI_{3n+1}$ (n = 3, 4, and 5) 2D perovskite films with vertical orientation and high crystallinity. The results expounded that the PCE of $(PEA)_2(MA)_4Pb_5I_{16}$ perovskite device was improved to 11.01% by optimizing the addition amount of NH_4SCN. Meanwhile, the oriented 2D perovskite film almost did not degrade after exposure to humidity (55 ± 5%) for 28 days. After being stored in the air with a humidity of 55 ± 5% for 160 h, the unsealed PSCs retained 78.5% of their original PCE (Fig. 4c).[35] This provided a highly efficient and stable new method for the commercialization of PSCs. Based on additive engineering, Yu *et al.* achieved high-efficiency and stable $(PEA)_2MA_3Pb_4I_{13}$ (n = 4) 2D RP PSCs at room temperature through the synergistic use of NH_4Cl additives and DMSO solvents. The research indicated that the PCE of the device can reach 13.41% with excellent air stability and eliminate hysteresis under the synergistic effect (Fig. 4d).[81] Li *et al.* effectively regulated the crystallization rate of $(PEA)_2(Cs)_{n-1}Pb_nI_{3n+1}$ during film deposition by adding the precursor additive *N*-methyl-2-pyrrolidone iodide (NMPI), which could form the hydrogen bonding (N–H···O) with DMAI to control the crystallization kinetics, thereby increasing carrier lifetime and reducing trap density (Fig. 4e).[82] The research achievements in crystallization kinetics opened up new avenues for the development of

2D RP PSCs. Zheng *et al.* developed a simple and multifunctional zwitterion (ZW) strategy for the preparation of highly efficient $(BA_{0.9}PEA_{0.1})_2MA_3Pb_4I_{13}$ 2D RP PSCs in ambient air. The findings revealed that ZW has a significant impact on the nucleation and crystallization kinetics of 2D RP perovskites, leading to a more desirable phase distribution and crystal orientation. Furthermore, it led to lower trap state density and enhanced charge transport properties, ultimately reaching a PCE of 17.04%, a V_{oc} of 1.19 V, and a J_{sc} of 18.93 mA cm^{-2} (Fig. 4f).[83] The performance of 2D RP PSCs with low *n* values based on the phenyl organic spacer cations represented by PEA are summarized in Table 2.[35,72,73,76–83]

Similar to the long-chain organic spacer cations, phenyl-based spacer cations have been extensively employed as surface passivation layers in 3D perovskite. Ghoreishi *et al.* used a series of phenylammonium derivatives: phenylammonium iodide (PAI), benzylammonium iodide (BAI) and PEAI to modify the $MAPbI_3$/Spiro-OMeTAD interface (Fig. 5a). The results showed that the 2D perovskite interfacial layers were formed on the surface of the $MAPbI_3$ film modified by PEAI and BAI, while a slightly different interfacial layer from 2D perovskite properties for PAI.[84] Zhu *et al.* gradually grew 2D nanosheets between the grain boundaries of the perovskite films, which significantly improved the humidity and thermal stability of the devices, inhibited the non-radiative charge recombination at the grain boundaries to achieve a PCE of 20.34%.[85] He *et al.* reported a simple strategy for precisely fabricating pure $n = 1$ 2D perovskite structure on 3D wide-bandgap (WBG) perovskites and achieving high PCE through low-temperature annealing. The effect of PEABr post-treatment on the bulk and surface of WBG perovskites and device performance was systematically demonstrated and revealed, ultimately yielding a high V_{oc} above 1.28 V for WBG PSCs with an E_g of 1.77 eV.[86] Liu *et al.* developed a gradient dimensional engineering technique that can passivate both bulk and interfacial defects in perovskite films. This approach involves the creation of a gradient 2D/3D heterojunction through the controlled diffusion of amphiphilic spacer cations from the interface to the bulk of the film, resulting in better defect passivation, improved hole extraction, and enhanced humidity stability (Fig. 5b). A PCE of 22.54% and a high V_{oc} of 1.186 V were obtained.[87]

In addition to the above-mentioned studies, many researchers are also studying the internal mechanism of 2D RP perovskites based on phenyl organic spacer cations. For example, Rebecca *et al.* studied the relationship between charge transport properties and crystal orientation with the ratio of MA^+ and PEA by mixing MA–PEA perovskite films. The result implied that the single-molecule charge carrier recombination rate first decreases with increasing PEA content, but then significantly increases as the exciton effect begins to dominate in the thin limiting layer (Fig. 5c).[88] It provides important ideas for reducing defect-related recombination and improving charge carrier migration rates. Cheng *et al.* investigated the effect of strain relaxation and residual strains on PEA and pentylamine (AA) 2D RP PSCs using X-ray diffraction and atomic force microscopy, which showed that the organic spacer cations can cause residual strains in the perovskite materials. By manipulating the composition of organic spacer cations, it was possible to control residual strains, leading to improved crystal quality, reduced recombination, enhanced charge transport, higher PCE, and significantly improved stability under conditions of temperature and humidity (Fig. 5d).[89] This research highlights the significance and effectiveness of strain relaxation and offers a straightforward approach for the reduction of residual strains in quasi-2D perovskites, which is an essential step towards commercialization for PSCs.

In general, the 2D RP perovskite films based on phenyl organic spacer cations represented by PEA are more moisture-resistant than 3D perovskites, and PEA 2D RP perovskite devices can be manufactured under environmental humidity conditions. The larger E_g of PEA 2D RP perovskites also makes them suitable as higher E_g absorbers in tandem devices. Compared with 3D PSCs, layered perovskite structures can provide greater tunability at the molecular level for material optimization. Compared with BA 2D RP PSCs, PEA 2D RP perovskite devices can exhibit better performance, which has made the 2D RP perovskites based on phenyl organic spacer cations represented by PEA become another core area of research.

3.3. 2D RP perovskites and devices based on the organic spacer cations containing F, Cl, and Br

The superior long-term stability of 2D RP PSCs, in comparison to their 3D devices, has gained significant interest. However, the integration of long-distance and large-size organic spacer cations can impede charge transport capabilities. Therefore,

Table 2 Performance summary of 2D RP PSCs (low *n* value) based on the phenyl organic spacer cations represented by PEA

Spacer	Strategy	Component	Stability	PCE (%)	Ref.
PEA	—	$(PEA)_2(MA)_2Pb_3I_{10}$	46 d humidity exposure, no severe breakdown	4.73	72
	Rb^+ doping	$(PEA)_2(MA)_4Pb_5I_{16}$	—	14.6	77
	BDA^{2+} additive	$(BDA)_{1-a}(PEA_2)_aMA_4Pb_5X_{16}$	95% of initial PCE under RH (40 ± 5%) for 500 h	17.21	78
	Gua^+ doping	$PEA_2(MA_{1-x}Gua_x)_2Pb_3I_{10}$	Enhanced stability after 750 h		79
	MAAc additive	$(PEA)_2(MA)_2Pb_3I_{10}$	—	5.7	80
	NH_4SCN additive	$(PEA)_2(MA)_4Pb_5I_{16}$	78.5% of initial PCE under RH (55 ± 5%) for 160 h	11.01	35
	NH_4Cl & DMSO additive	$(PEA)_2MA_3Pb_4I_{13}$	Good environmental stability	13.41	81
	NMPI additive	$(PEA)_2(Cs)_{n-1}Pb_nI_{3n+1}$ ($n = 20$)	Unsealed, PCE ≈ 92.7% after 30 d	14.59	82
	ZW additive	$(BA_{0.9}PEA_{0.1})_2MA_3Pb_4I_{13}$	Over 93% of initial PCE after 720 h aging at room temperature	17.04	83
PBA	—	$(PBA)_2Cs_{n-1}Pb_nI_{3n+1}$	RH = 20–80% ± 5% over 450 d	—	73
PhFA	—	$(PhFA)_2MA_{n-1}Pb_nI_{3n+1-x}Cl_x$ ($n = 5$)	Significantly improved stability	17.37	76

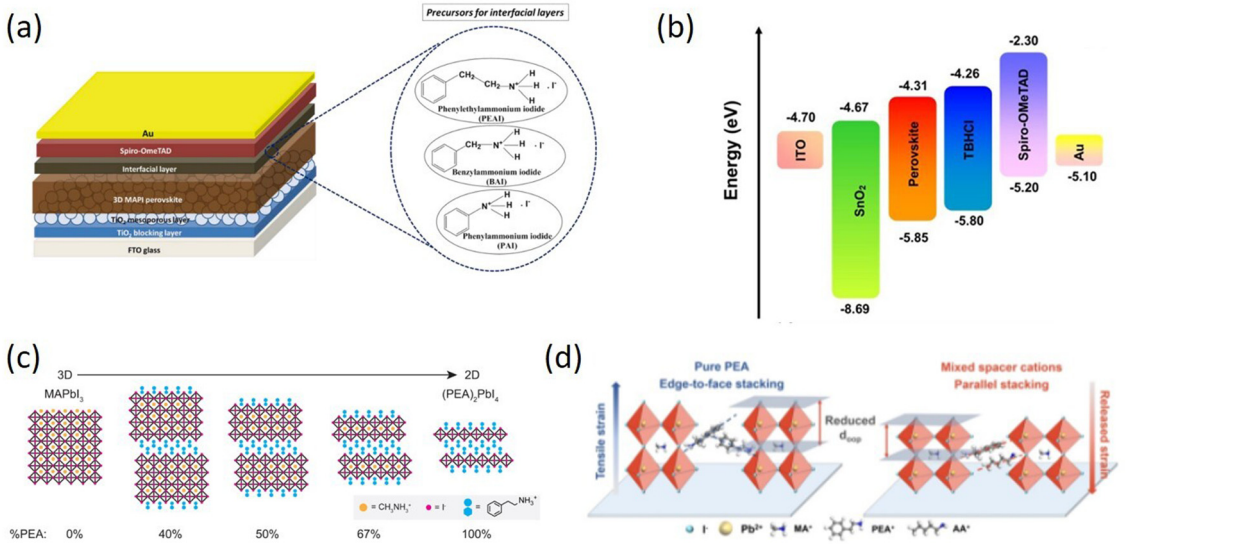

Fig. 5 (a) Schematic structure of PSCs with three different interfacial layers and the corresponding molecular structures of the precursors (PEAI, BAI, and PAI, respectively). Adapted from ref. 84 with permission. Copyright 2020, Elsevier. (b) Energy-level diagram of the device components. Adapted from ref. 87 with permission. Copyright 2022, American Chemical Society. (c) Schematic crystal structures of $MAPbI_3$, $(PEA)_2PbI_4$, and intermediate mixed MA–PEA 2D perovskites. Adapted from ref. 88 with permission. Copyright 2016, American Chemical Society. (d) Schematic illustration of strain relaxation by introducing mixed spacer cations, and oop means out-of-plane. Adapted from ref. 89 with permission. Copyright 2022, Wiley.

more and more studies have focused on further design of organic spacer cations and chemical regulation of spacer cations has been proven to be an effective and easy way to improve charge transport efficiency in 2D perovskites.[90] Organic spacer cations with halogens (F, Cl, and Br), such as $CF_3CF_2CH_2NH_3^+$ (5F-PA$^+$),[91] *p*-fluoraniline (FAL),[92] selective monofluorination of PEA (oF1PEA, mF1PEA, and pF1PEA),[93] fluorinated PEA (FPEA)[94] are a new type of high-performance compounds developed by scientists.

Among various organic cations with halogen, the research on organic cations with F is the most extensive due to its high dipole moment and strong hydrophobicity. Hu *et al.* investigated how the chemical properties of organic cations affect the performances of 2D perovskite materials and devices. Selective monofluorination of PEA (oF1PEA, mF1PEA, and pF1PEA) at different positions of the phenyl ring can significantly affect the PCE of these 2D PSCs (n = 4). The 2D PSCs based on pF1PEA showed the highest PCE of 10.55%, followed by mF1PEA (10.17%), PEA (7.67%), and oF1PEA (less than 1%). These findings offer insights for designing organic cations and comprehending intermolecular interactions associated with such organic cations (Fig. 6a).[93] Shi *et al.* developed a new fluorinated PEA to prepare quasi-2D $(4FPEA)_2(MA)_4Pb_5I_{16}$ (n = 5) PSCs and successfully improved the performance of 2D PSCs, achieving a high PCE of 17.3% and stability, which is attributed to the critical role of fluorination in film morphology, defect density, mixed-phase distribution and charge dissociation kinetics (Fig. 6b).[94] Paek *et al.* created a highly hydrophobic cation, perfluoroalkyl iodide (5FBzAI), and utilized it to design a 2D perovskite material with enhanced intermolecular interactions. The use of 5FBzAI resulted in improved interface passivation, reduced charge recombination, and enhanced stability of photovoltaic devices, outperforming the benchmark 2D system. Under the impact of strong halogen bond, $(5FBzAI)_2PbI_4$ capping layer displayed in-plane crystal orientation, leading to a high PCE of 21.65% for PSCs.[95]

As the focus on organic spacer cations with F has intensified, scientists have also proposed spacer cations containing other halogens. For example, Li *et al.* first applied the novel 4-chlorophenylformamide (CPFA) organic spacer cation in quasi-2D RP PSCs and used MACl to promote crystal growth and orientation of the perovskite film. High-quality quasi-2D $CPFA_2MA_{n-1}Pb_n(I_{0.857}Cl_{0.143})_{3n+1}$ (n = 9) perovskite films were formed, which showed improved crystal orientation, reduced trap density, prolonged carrier lifetime, optimized energy level alignment, and a maximum PCE of 14.78% with significantly improved environmental stability.[96] Liu *et al.* also introduced 4-chlorobenzylammonium (CBA) as the second spacer cation in $(HEA)_2(Cs_{0.1}FA_{0.9})_8Pb_9(I_{0.95}Br_{0.05})_{28}$ (HEA is ethanol ammonium). Due to the passivation effect of CBA, the performances of PSCs were significantly improved with the highest PCE of 18.75% (Fig. 6c).[97] They also systematically studied the effects of small-sized alkylammonium salts on the properties of 2D/3D perovskites. By introducing suitable hydrophobic 2-chloroethylamine hydrochloride (CEA-Cl) and 2-bromoethylamine hydrobromide (BEA-Br) into FA-based 3D perovskites, the devices with 5% CEA-Cl showed a PCE of 20.08% with improved stability (Fig. 6d).[98] The performance of 2D RP PSCs based on the organic spacer cations containing F, Cl, and Br are summarized in Table 3.[91–98]

From the above studies, it can be seen that the 2D RP perovskites based on the spacer cations with halogens generally have superior performances. However, their specific effects on 2D perovskites are not clear; thus, the researchers have

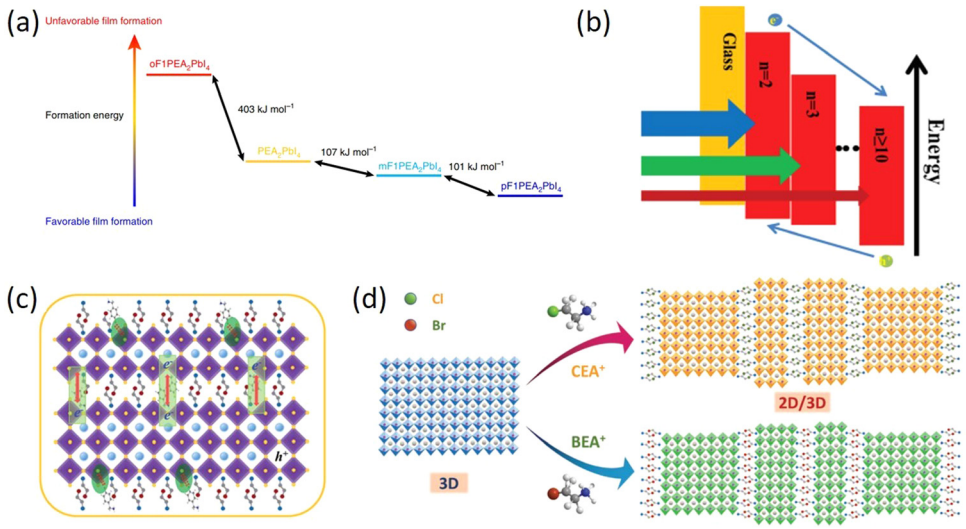

Fig. 6 (a) Relative formation energy difference between different 2D OIHPs (n = 1). DFT calculation of formation energy for PEA_2PbI_4, $oF1PEA_2PbI_4$, $mF1PEA_2PbI_4$, and $pF1PEA_2PbI_4$. Adapted from ref. 93 with permission. Copyright 2019, Springer Nature. (b) Energy-level alignment of RPP film with different n values. Adapted from ref. 94 with permission. Copyright 2019, Wiley. (c) Schematic illustration of the process of promoting the improvement of quasi-2D perovskite performance after the incorporation of CBA and FBA. Adapted from ref. 97 with permission. Copyright 2020, Royal Society of Chemistry. (d) Schematic illustration of the self-assembled 2D/3D perovskite structure. Adapted from ref. 98 with permission. Copyright 2019, Wiley.

Table 3 Performance summary of 2D RP PSCs based on the organic spacer cations containing F, Cl, and Br

Spacer	Component	Stability	PCE (%)	Ref.
5F-PA	$5F\text{-}PA_{0.05}[Cs_{0.05}(MA_{0.17}\ FA_{0.83})_{0.95}]_{0.95}Pb(Br_{0.17}I_{0.83})_3$	80% of initial PCE under RH (65 ± 10%) for 300 h	22.8	91
FAL	$FBA_2MA_{n-1}Pb_nI_{3n+1}$	After light for 1000 h, no decomposition	20.48	92
mF1PEA or pF1PEA	$(mF1PEA)_2(MA)_3Pb_4I_{13}$ or $(pF1PEA)_2(MA)_3Pb_4I_{13}$	—	10.55	93
FPEA	$(4FPEA)_2(MA)_4Pb_5I_{16}$	Unsealed, excellent humidity and thermal stability	17.3	94
5FBzAI	$Cs_{0.1}(FA_{0.86}MA_{0.14})_{0.9}Pb(I_{0.86}Br_{0.14})_3$ with $(5FBzA)_2PbI_4$ capping layer	Extended stability after 1100 h of continuous lighting	21.68	95
CPFA	$CPFA_2MA_{n-1}Pb_n(I_{0.857}Cl_{0.143})_{3n+1}$ (n = 9)	80% of initial PCE after 2000 h under environmental conditions	14.78	96
CBA	$(HEA_{0.9}CBA_{0.1})_2(Cs_{0.1}FA_{0.9})_8Pb_9(I_{0.95}Br_{0.05})_{28}$ (0.1CBA)	RH = 45 ± 5% air after 1500 h, 90% of initial PCE	18.75	97
BEA-Br	$(Cs_{0.1}FA_{0.9})Pb(I_{0.9}Br_{0.1})_3$	RH 50 ± 5% air after 2400 h, 92% of initial PCE	20.08	98

compared and studied in detail the impact of different halogens or different halogen numbers of substitution in the spacer cations. Wang *et al.* conducted an in-depth study on the effects of halogen substitution on the crystal orientation and multi-phase distribution of PEA 2D perovskite films. By fine-tuning the spacer cation, the humidity and thermal stability of 2D RP PSCs can be improved, which is caused by the halogen eliminating the n = 1 2D perovskite, resulting in a vertical crystal orientation. Halogen-substituted PEA perovskites have a crystal orientation perpendicular to the substrate, which is beneficial for vertical charge transfer. There is nucleation competition between the small n phase and large n phase in PEA and X-PEA-based perovskites, which results in the ordered distribution of different n phases in PEA and F-PEA 2D perovskite films, while the random distribution in Cl-PEA and Br-PEA films (Fig. 7a). The PCE of $(F\text{-}PEA)_2MA_3Pb_4I_{12}$ (n = 4) devices is 18.10%, which significantly higher than that of PEA (12.23%), Cl-PEA (7.93%), and Br-PEA (6.08%). This work provides a convenient method to improve the performance of PSCs by adjusting the structure of organic spacer molecules.[97] Fu *et al.* demonstrated for the first time the introduction of strong chemical interactions (halogen–halogen bonding) at the phase interface to suppress ion migration by increasing the corresponding activation energy. Various characterizations showed that the formed halogen–halogen bonds between 2D and 3D phases suppressed halide segregation. The constructed series of halide 2D perovskites ($(I\text{-}FEA)_2PbI_4$, $(Br\text{-}FEA)_2PbI_4$, $(Cl\text{-}FEA)_2PbI_4$, $(F\text{-}FEA)_2PbI_4$) were introduced into 3D WBG $CsMAFAPb(I_xBr_{1-x})_3$ perovskite, which exhibited a PCE of 19.19%. Importantly, the suppressed ion migration enhanced the long-term operational stability of the devices (Fig. 7b).[100] Wang *et al.* prepared $(F_xPEA)_2PbI_4$ (x = 1, 2, 3, and 5) 2D perovskites by using 4-fluorophenethylamine iodide, 3,5-difluorophenethylamine iodide, 2,4,5-trifluoroethylphenethylamine iodide, and 1,2,3,4,5-pentafluorophenethylamine iodide to systematically study the effect of fluorination degree on the resulting 2D/3D perovskite. The PCEs were, respectively, increased from 20.75% for the control device to 21.09%, 22.06%, 22.74%, and 21.86%, and the humidity stability

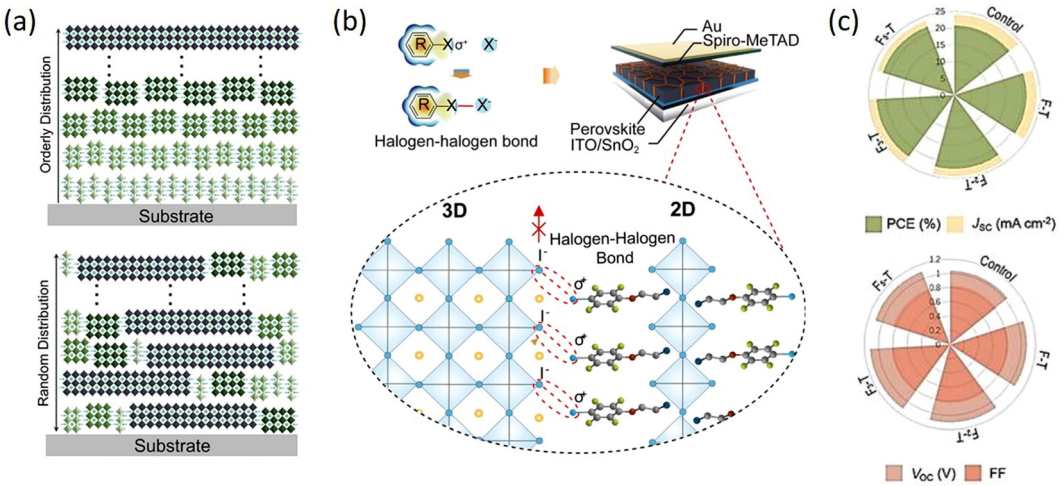

Fig. 7 (a) Schematic illustrations to indicate Q-2D RP perovskites with orderly and random *n*-phases distribution. Adapted from ref. 99 with permission. Copyright 2020, Wiley. (b) Schematic diagram of interfacial halogen–halogen bonded 2D/3D hybrid perovskites. Adapted from ref. 100 with permission. Copyright 2021, Elsevier Inc. (c) Photovoltaic parameters of 2D/3D PSCs with FPEAI, F2PEAI, F3PEAI, and F5PEAI cations compared to the control device. Adapted from ref. 101 with permission. Copyright 2022, Elsevier BV.

was improved with the increasing fluorination degree of aromatic cations (Fig. 7c).[101]

Currently, 2D perovskite passivation layers based on the halogen-substituted spacer cations have been studied more and more and shown great potential. Zhao *et al.* found that 4-fluoroaniline (FAL) not only has non-destructive surface passivation but also has large molecular dipoles to induce charge transfer. The aromatic ring and *p*-fluorinated conjugate amines reduced the basicity to allow FAL as an anti-solvent for perovskites over a wider range of temperatures and time. The stability and photovoltaic performances of PSCs with hydrophobic fluorine tails are improved by molecular passivation to form an ultra-thin protective layer. Finally, the PCE of FAL-passivated PSCs was 20.48% and stability was also improved under environmental conditions.[92] Liu *et al.* designed four LD perovskite coverage layers based on different halogen-substituted benzylammonium aromatic cations to achieve high-performance devices. Four 2D perovskites exhibited different crystal parameters and chemical properties, leading to suppressed non-radiative recombination and decreased trap density. The BBAI-modified devices achieved the highest PCE of 21.13%.[102] Wang *et al.* proposed to introduce BACl and PbI_2 at the top of the SnO_2 ETL to modify the ETL/perovskite interface. Their research showed that the 2D interface composed with BACl: PbI_2 simultaneously passivated defects at the ETL/perovskite interface, and improved the electronic characteristics of the ETL. The quality of crystalline perovskite film was improved by promoting charge separation/collection and suppressing interface recombination due to favorable energy alignment of the interface layer, which resulted in a PCE of 21.15%.[103]

The incorporation of organic spacer cations with halogen into 2D perovskites can not only effectively improve their environmental stability, but also induce the crystal structure change to better modify the energy levels. Changing the type and ratio of organic spacer cations with halogen to fine-tune device performance is a promising approach. Although the incorporation of organic spacer cations with halogen has many positive effects, excessive halogen can cause lattice distortion, hinder charge transfer, and the surface halogen is also easy to react with water and oxygen in the environment, thus affecting the stability and performance of 2D RP PSCs. Therefore, the use of organic spacer cations with halogen still needs to be further explored to effectively address these challenges.

3.4. 2D RP perovskites and devices based on the heterocyclic organic spacer cations containing N, S, and other heteroatoms

Appropriate organic spacer cations with special structures have an important impact on the performances and stability of PSCs because different functional groups in organic spacer cations can interact with perovskite components, such as hydrogen bonds between OH^- and ammonium salt cations, Lewis acid–base interaction between electron pairs in S, N, O and uncoordinated Pb^{2+} in perovskite.[104,105] Therefore, it is necessary to introduce new heterocyclic organic spacer cations containing N, S, and other heteroatoms to obtain new 2D perovskites, and then 2D RP perovskite materials based on such organic spacer cations gradually come into people's vision.

As is known, integrating 3D perovskite with 2D RP can maintain the advantages of both components. Yan *et al.* introduced thiazol-2-amine (TEA) with sulfur as an organic lattice spacer and stabilizer to form $TEA_2MA_3Pb_4I_{13}$ perovskite, demonstrating the spontaneous formation of the 3D phase embedded in a 2D perovskite matrix at room temperature. The formation of a 2D/3D bulk heterojunction structure was proposed to be a result of compressive strain-induced epitaxial growth of the 3D phase at the grain boundary of the 2D phase through Pb–S interaction (Fig. 8a). Compared with typical PEA-2D perovskite, the prepared TEA 2D perovskite exhibited longer exciton diffusion length and extended charge carrier lifetime, thereby demonstrating excellent PCE of 7.20% and significantly

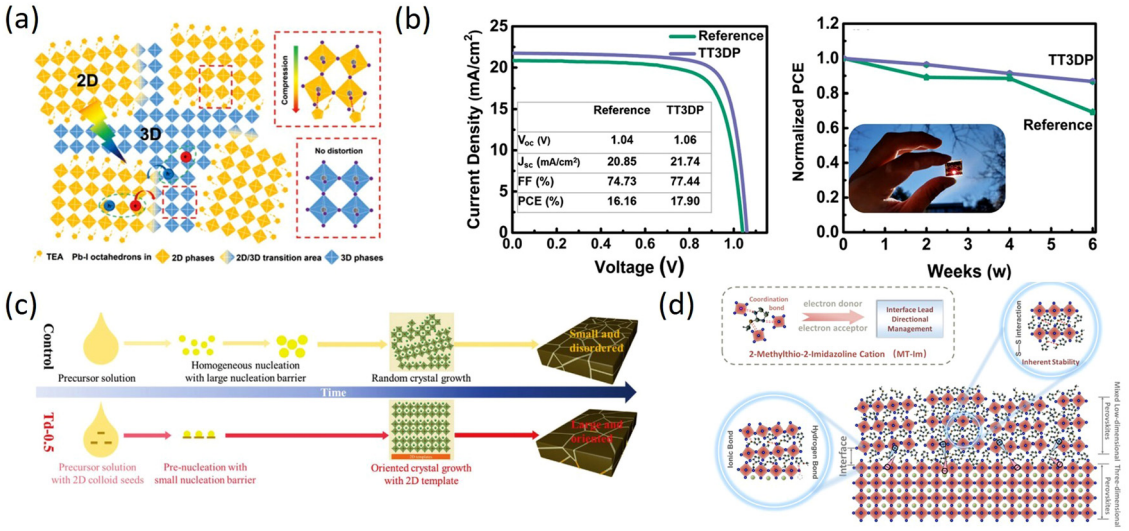

Fig. 8 (a) Schematic illustration of 2D/3D mixed phases in TEA perovskites. Adapted from ref. 106 with permission. Copyright 2019, Wiley. (b) *J*–*V* curves of the champion reference and TT3DP ST-PSCs and normalized PCE of the reference and TT3DP ST-PSCs kept under the dark at room temperature with <15% relative humidity. Adapted from ref. 108 with permission. Copyright 2021, Wiley. (c) Schematic diagram of the film crystallization process of control and Td-0.5 films. Adapted from ref. 109 with permission. Copyright 2022, Wiley. (d) Schematic illustration of the effective management by inherently stable MT-Im LDP for the Pb-based defects at the interface. Adapted from ref. 110 with permission. Copyright 2021, American Chemical Society.

increased J_{sc}.[106] Dong *et al.* successfully synthesized 2-thiophenemethylamine (ThFA, a derivative of FA) and used it as an organic spacer to prepare high-quality $(ThFA)_2(MA)_{n-1}Pb_nI_{3n+1}$ 2D perovskite films by precursor organic salt-assisted crystal growth technology. The vertical growth orientation was preferred in the films, along with reduced trap density and high charge carrier mobility. Consequently, the inverted planar p–i–n structure of 2D RP PSCs exhibited markedly enhanced PCE from 7.23% to 16.72% with excellent stability.[107] Gunes *et al.* synthesized organic cation (TTMAI) based on thienothiophene to treat 3D perovskite. Detailed analysis showed that a 2D (n = 1) or quasi-2D layer was formed on the surface of PbI_2-rich 3D perovskite. The TTMAI-treated device exhibited improved FF and increased PCE from 17% to over 20%. Drift-diffusion simulations illustrated that the enhancement resulted from better hole extraction. In addition, due to the hydrophobicity of TTMAI, the stability of the device was also improved (Fig. 8b).[108] Wang *et al.* prepared 3D perovskite films with high crystal orientation and large grain sizes using a 2D perovskite template of thiourea 1,1-dioxide iodine lead (Td_2PbI_4) and a bottom-up growth method. The addition of TdCl to the precursor solution facilitated the accumulation of pre-crystallized 2D Td_2PbI_4 seeds at the bottom interface, which lowered the nucleation barrier and improved the (100) orientation, resulting in a reduction of defects during template-directed crystallization of 3D perovskite film growth (Fig. 8c). Based on this, the Td-0.5PSC displayed a PCE of 22.09% with a V_{oc} of 1.16 V and high stability.[109] The presence of Pb–I anti-site and uncoordinated Pb^0 defects at the interface can impact both the PCEs and the stability of PSCs. Managing Pb-based defects in a specific orientation can lead to a reduction in defect density and voltage loss, ultimately improving PCE and stability. Therefore, Liu *et al.* proposed a strategy for designing a low-dimensional perovskites (LDP) passivation layer using an amphoteric heterocyclic cation (2-methylthio-2-imidazolinium, MT-Im). The study demonstrated that MT-Im can passivate both positive and negative Pb-based defects, resulting in increased defect formation energy for Pb–I anti-site defects. Moreover, MT-Im can suppress the production of Pb^0 by interacting with uncoordinated Pb^{2+} (Fig. 8d). Ultimately, the device achieved a PCE of over 24% with negligible hysteresis and exhibited long-term humidity and high-temperature stability.[110] Sutanto *et al.* used new thiophene-based ammonium organic cations, 2-thiophenemethylammonium iodide (2-TMAI), 3-thiophenemethylammonium iodide (3-TMAI), and 2-thiopheneethylammonium iodide (2-TEAI) as building blocks for 2D perovskites on 3D perovskite films to observe the slow evolution of 2D/3D PSCs performances and the impact on the PCE and stability. They found that the 2D/3D interface is inherently dynamic, which can act as an ion scavenger and self-transform into a quasi-2D gradient interface under aging or thermal stress. In addition, the deposition of 2D layers with various thiophene-based ammonium cations protected the 3D layer from degradation in ambient air.[111] Salado developed three passivators (MIC2, MIC3, MIC4) using substituted thiazole iodides (TMI) to prepare perovskite devices. The TMI-based 2D interfacial layer functionalized the surface and enhanced hydrophobicity. TMI treatment led to enhanced V_{oc} and FF by reducing possible recombination paths at the perovskite/hole-selective interface, owing to the reduced shallow and deep traps. Additionally, TMI-passivated perovskite layers significantly reduced degradation caused by humidity and MA^+ thermal diffusion.[112] The performance of 2D RP PSCs based on the heterocyclic organic spacer cations containing N, S, and other heteroatoms are summarized in Table 4.[106–112]

Organic spacer cations containing N, S, and other heteroatoms can provide additional bonding sites and enhance the structural stability of 2D RP perovskites, which show great

Table 4 Performance summary of 2D RP PSCs based on the heterocyclic organic spacer cations containing N, S, and other heteroatoms

Spacer	Component	Stability	PCE (%)	Ref.
TEA	$TEA_2MA_3Pb_4I_{13}$	80% of initial PCE under RH (60 ± 5%) for 270 h	7.20	106
ThFA	$(ThFA)_2(MA)_{n-1}Pb_nI_{3n+1}$ (n = 3)	Unsealed, N_2, 99% of initial PCE for 300 h	16.72	107
TTMAI	$(FAPbI_3)_{1-x}(MAPbBr_3)_x$	RH 15%, 82% of initial PCE after 380 h	20	108
TdCl	$Cs_{0.05}FA_{0.8}MA_{0.15}Pb(I_{0.9}Br_{0.1})_3$	N_2, 84% of initial PCE for 500 h	22.09	109
MT-Im	$(Cs_{0.03}FA_{0.97}PbI_3)_{0.95}(MAPbBr_3)$	Excellent stability	24.07	110
TMAI & TEAI	$[(FAPbI_3)_{0.87}(MAPbBr_3)_{0.13}]_{0.92}$ $(CsPbI_3)_{0.08}$	—	Over 20	111
TMI	$(FAPbI_3)_{0.97}(MAPbBr_3)_{0.03}$	RH 50%, 95% of initial PCE after 800 h	18.93	112

promise in improving device performance. The introduction of heteroatoms in 2D RP perovskites has been shown to be an effective strategy to regulate the band structure and precisely controlling the type and proportion of heteroatoms can also adjust the carrier lifetime and diffusion length of the 2D RP perovskite films, thereby further improving the performance. Despite these significant advances, there is still room for improvement and optimization. The selection and number of heteroatoms such as N and S have a considerable impact on the performance of 2D RP perovskites, and finding the best way to incorporate them into perovskite structures is also a challenge. In addition, the current methods used to synthesize these organic spacer cations containing N, S, and other heteroatoms are expensive and complex, thus there is a need to develop easier and more cost-effective synthesis methods to scale up their applications.

3.5. 2D RP perovskites and devices based on other organic spacer cations

The selection of organic cations has a great impact on the crystal structure and physical properties of 2D perovskites, which is the main factor determining the quality of light-absorbing layers and the PCEs of 2D PSCs. Therefore, it is necessary to develop other spacer cations to expand the 2D perovskite family and explore its application in PSCs. 2D perovskites have only appeared for a few years, and more and more spacer cations have been developed. Except for BA, PEA, heterocyclic ring, and its derivatives summarized above, other spacer cations have also been studied a lot and achieved great success, such as butylammonium acetate (BAAcO),[113] glycine salt,[114] 4-amino-1-butanol hydroiodide (4ABI),[115] 4-hydroxybenzamidine hydrochloride (*p*-HOPhFACl),[116] and 4-(aminomethyl) benzoic acid hydrogen bromide (ABHB).[117] The performance of 2D RP PSCs based on other organic spacer cations is summarized in Table 5.[51,113–117]

Among these spacer cations, many typical representatives have played important roles in the development of 2D RP PSCs. For example, Qiu *et al.* reported an ionic liquid spacer (BAAcO) to construct highly efficient and stable tin-based 2D RP PSCs. AcO^- in BAAcO has strong interactions with FA^+ and Sn^{2+}, which is in sharp contrast to traditional halide ammonium spacer (BAI) (Fig. 9a). The interactions between the components can form controllable intermediates, which facilitate the growth of smooth, dense, and highly oriented perovskite films. The resulting PCE is 10.36% and the stability has also been improved.[113] Zheng *et al.* first proposed a new self-additive 2D RP perovskites with high photovoltaic performances by introducing glycine salts (GlyCl) with prominent additive effects. The interaction between Pb^{2+} and C=O in Gly made Gly become a favorable nucleation center, which promoted uniform and rapid growth of large-grain Gly-based RP perovskites, leading to reduced grain boundaries and improved charge carrier transport characteristics. The results showed that 2D RP PSCs exhibit excellent photoelectric performances with the PCEs of 18.06% for Gly (n = 8) and 15.61% for Gly (n = 4), as well as long-term stability under humidity, heat, and UV light (Fig. 9b).[114] Ma *et al.* proposed a method to improve the moisture resistance of perovskites by surface-treating the perovskite films with hydrophilic 2-aminoethanol hydrogen iodide (2AEI) or 4-aminobutanol hydrogen iodide (4ABI). The hydrophilic materials used for post-treatment effectively protected the underlying perovskite layer from moisture and surface passivation reduced the surface trap density by interacting with the mismatched lead and iodide centers (Fig. 9c). Ultimately, the PSCs displayed a PCE of 23.25%.[115] Liu *et al.* developed a class of aromatic methylimidazolium (ArFA) as spacer cations for 2D/3D perovskites. The study revealed that there existed multiple NH···I hydrogen bond interactions between large aromatic spacer ArFA and inorganic $[PbI_6]^{4-}$ layers in 2D/3D perovskite structures. These interactions can promote crystal growth and orientation, reduce defect states and improve carrier lifetimes. As a result, the 2D/3D perovskite devices based on phenylmethylimidazolium chloride (PhFACl) exhibited a PCE of 22.39% and long-term thermal stability

Table 5 Performance summary of 2D RP PSCs based on other organic spacer cations

Spacer	Component	Stability	PCE (%)	Ref.
BAAcO	$(BA_{0.3}PEA_{0.7})_2FA_3Sn_4I_{13}$ (n = 4)	Unsealed, N_2, 90% of initial PCE for 600 h	10.36	113
Gly	$[Gly_2(Cs_{0.05}FA_{0.95})_{n-1}Pb_nI_{3n-1}Cl_2]_{0.9}(FAPbBr_3)_{0.1}$ (n = 8)	94% of initial PCE for 1920 h	18.06	114
2AEI&4ABI	$FAPbI_3$	90% of initial PCE under RH = 20% for 1000 h	23.25	115
ArFA	sequential vapor deposition	Long-term thermal stability	22.39	116
ABHB	$MAPbI_3$	Enhanced environmental stability	21.18	117
CHA_2PbI_4 & $CHMA_2PbI_4$	$FAPbI_3$	—	23.91	51

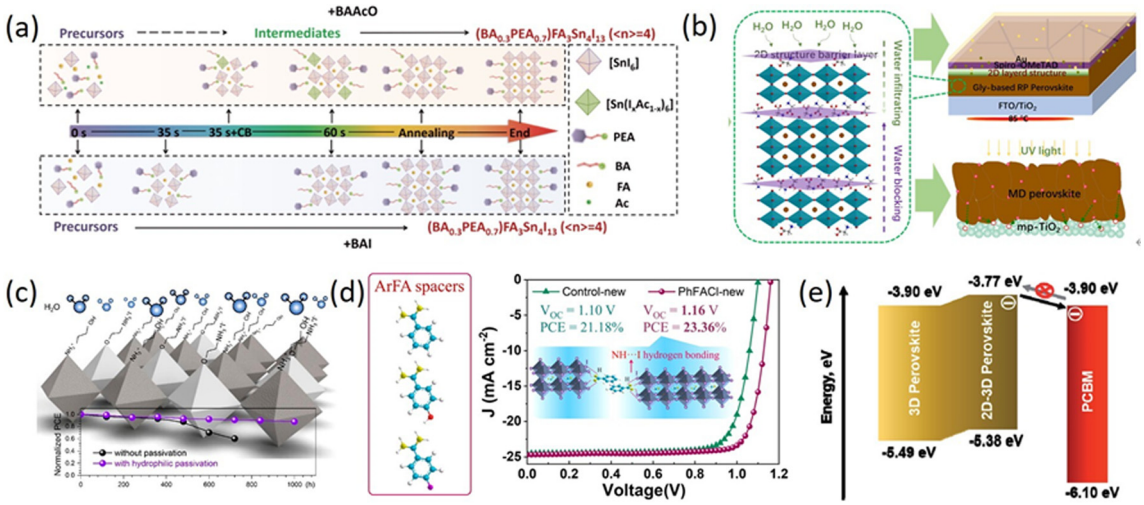

Fig. 9 (a) Schematic diagram of the crystallization process of 2DRP Sn-based perovskites based on +BAAcO and +BAI (color online). Adapted from ref. 113 with permission. Copyright 2021, Science China Press. (b) The mechanism process for enhanced moisture, thermal, and UV light stability. Adapted from ref. 114 with permission. Copyright 2020, Wiley. (c) Schematic illustration of hydrophilic passivation layers and stability tests of PSCs with and without hydrophilic passivation. Adapted from ref. 115 with permission. Copyright 2020, American Chemical Society. (d) Chemical structure of spacer cations PhFA, *p*-HOPhFA, and *p*-FPhFA, schematic diagram of corner-sharing $[PbI_6]^{4-}$ octahedrons layers interaction with ArFA spacers through hydrogen bonding and *J*–*V* curves of the devices based on control 3D and 2D/3D perovskites. Adapted from ref. 116 with permission. Copyright 2021, American Chemical Society. (e) Energy-level alignment at the perovskite and PCBM interface. Adapted from ref. 117 with permission. Copyright 2021, Royal Society of Chemistry.

(Fig. 9d).[116] Garai *et al.* demonstrated the potential for surface recrystallization of 2D-3D gradient perovskites prepared by surface treatment of multifunctional ABHB. Br^- filled the halide vacancies in the perovskite lattice, while –NH and –COOH functional groups significantly minimized defect states and reduced ion migration (Fig. 9e). Therefore, ABHB-treated PSCs displayed outstanding PCEs of 21.18% for 0.12 cm^2 and 18.81% for 2 cm^2 with negligible hysteresis. Due to the improved hydrophobicity, the covered 2D layer restricted moisture infiltration into the perovskite layer and dramatically enhanced the environmental stability of PSCs.[117] Jeong *et al.* introduced novel 2D layered perovskites, such as CHA_2PbI_4 (CHAI = cyclohexylammonium iodide) and $CHMA_2PbI_4$ (CHMAI = cyclohexylmethyl ammonium iodide) into the interface between 3D perovskite structures and the hole transport layer by a simple solution method, forming and verifying the 2D/3D perovskite heterojunction structure. Spontaneous electroluminescence quenching was observed owing to the effective hole extraction and good valence band alignment. Transient photocurrent and photovoltage measurements were conducted to directly assess the charge extraction and recombination abilities. As a result, the device with 2D/3D perovskite heterojunction exhibited a PCE from 20.41% to 23.91%.[51]

Despite extensive research on the 2D RP perovskites based on BA and PEA, there is currently no agreement on the best choice for organic spacer cations and researchers are actively exploring new and replaceable organic spacer cations. Several effective organic spacer cations mentioned above, including BAAcO and Gly, display positive effects, but further research is needed to determine how to select the appropriate spacer cation type and adjust the spacer position to achieve the best device performance. In addition, exploring alternative spacer cations while employing more effective strategies, such as component regulation, additive engineering, ion doping, and 2D/3D heterojunction construction, is critical to improving the thermal stability and PCE of 2D RP PSCs.

4. Summary and future prospects of 2D RP perovskites

In recent years, 2D RP PSCs have achieved significant improvement in PCE while maintaining high stability. Researchers have prepared 2D RP perovskite devices with high PCE and superior stability by adopting various effective strategies, such as composition regulation, additive introduction, and 2D perovskite interface layers, which make them become the most promising perovskite materials currently. However, the performances still need to be further improved beyond that of 3D PSCs to be competitive. Therefore, there is still a long way to go from theoretical research to practical application for 2D RP PSCs based on the low *n* value.

Looking ahead, the further development of 2D RP PSCs still faces significant challenges. Firstly, the formation mechanism of 2D layered perovskites is not yet well understood, especially for materials based on different spacer cations, which have more diverse compositions and properties, making their formation mechanisms more complex. These spacer cations also affect the charge transfer, crystal structure, and phase distribution of 2D RP perovskites. The low conductivity of organic isolated cations will hinder the effective charge transfer in the photoelectric device and reduce the short circuit current. The

incorporation of a large number of organic spacer cations will distort the lattice structure and lead to the mismatch of the dielectric properties of the 2D RP perovskite structure. In addition, 2D RP perovskites often present a complex structure with different mixed phases, and the composition and distribution of the 2D phase can also change the performance of PSCs. Therefore, conducting detailed mechanistic studies to understand the impact of organic spacer cations on 2D perovskite performances is critical for designing more high-performance and high-stability 2D RP perovskites. Secondly, most stability research currently relies on single or laboratory-created aging conditions. Although 2D RP perovskites have higher stability than 3D perovskites, there are not many studies on the stability under multi-factor or actual operating conditions, and the stability results are not ideal. To meet the requirements of practical applications, further studies and enhancements are required for the long-term stability of 2D RP perovskite devices. At the same time, to realize the industrialization of 2D RP PSCs, the biggest problem is their large-scale preparation, which is rarely reported. To maintain high PCEs for large-area 2D RP PSCs, it is important to maintain the uniformity and density of 2D RP perovskite films. However, their performances are still far from the requirements of large-area 2D RP PSCs, which is needed to be further improved. Overall, this is a very promising field for research, and it is believed that the 2D RP perovskites will break through various challenges and achieve more excellent results in the near future with the unremitting efforts of scientific researchers all over the world, and ultimately promote the commercialization of PSCs.

Author contributions

H. Zheng and G. Liu proposed the topic, designed the framework, and completed the final article. C. Wang wrote the first draft of this review, revised it according to the questions and suggestions, and drew the tables and figures in this review. X. Dong arranged the required references and selected suitable figures from the references to incorporate into the article. F. Chen checked and revised the overall format of this review and obtained copies of permissions from other publishers to reproduce the figures shown in the article.

Conflicts of interest

The authors declare no conflicts of interest.

Acknowledgements

This work was financially supported by the National Natural Science Foundation of China (grant 52102196) and the University Synergy Innovation Program of Anhui Province (GXXT-2022-009).

References

1 G. Xing, N. Mathews, S. Sun, S. S. Lim, Y. M. Lam, M. Grätzel, S. Mhaisalkar and T. C. Sum, Long-range balanced electron- and hole-transport lengths in organic-inorganic $CH_3NH_3PbI_3$, *Science*, 2013, **342**, 344–347.
2 Q. Lin, A. Armin, R. C. R. Nagiri, P. L. Burn and P. Meredith, Electro-optics of perovskite solar cells, *Nat. Photonics*, 2014, **9**, 106–112.
3 A. Marchioro, J. Teuscher, D. Friedrich, M. Kunst, R. vande Krol, T. Moehl, M. Grätzel and J.-E. Moser, Unravelling the mechanism of photoinduced charge transfer processes in lead iodide perovskite solar cells, *Nat. Photonics*, 2014, **8**, 250–255.
4 L. Protesescu, S. Yakunin, M. I. Bodnarchuk, F. Krieg, R. Caputo, C. H. Hendon, R. X. Yang, A. Walsh and M. V. Kovalenko, Nanocrystals of Cesium Lead Halide Perovskites (CsPbX3, X = Cl, Br, and I): Novel Optoelectronic Materials Showing Bright Emission with Wide Color Gamut, *Nano Lett.*, 2015, **15**, 3692–3696.
5 A. Kojima, K. Teshima, Y. Shirai and T. Miyasaka, Organometal halide perovskites as visible-light sensitizers for photovoltaic cells, *J. Am. Chem. Soc.*, 2009, **131**, 6050–6051.
6 **https://www.nrel.gov/pv/cell-efficiency.html**.
7 J. W. Lee and N. G. Park, Chemical Approaches for Stabilizing Perovskite Solar Cells, *Adv. Energy Mater.*, 2020, **10**, 1903249.
8 E.-B. Kim, M. S. Akhtar, S. Ameen, A. Umar, H. Qasem, H.-G. Rubahn, M. Shkir, A. Kaushik and Y. K. Mishra, Improving the performance of 2D perovskite solar cells by carrier trappings and minifying the grain boundaries, *Nano Energy*, 2022, **102**, 107673.
9 H. Tsai, W. Nie, J. C. Blancon, C. C. Stoumpos, R. Asadpour, B. Harutyunyan, A. J. Neukirch, R. Verduzco, J. J. Crochet, S. Tretiak, L. Pedesseau, J. Even, M. A. Alam, G. Gupta, J. Lou, P. M. Ajayan, M. J. Bedzyk and M. G. Kanatzidis, High-efficiency two-dimensional Ruddlesden-Popper perovskite solar cells, *Nature*, 2016, **536**, 312–316.
10 J. Yan, W. Qiu, G. Wu, P. Heremans and H. Chen, Recent progress in 2D/quasi-2D layered metal halide perovskites for solar cells, *J. Mater. Chem. A*, 2018, **6**, 11063–11077.
11 Z. Wang, Q. Lin, F. P. Chmiel, N. Sakai, L. M. Herz and H. J. Snaith, Efficient ambient-air-stable solar cells with 2D-3D heterostructured butylammonium-caesium-formamidinium lead halide perovskites, *Nat. Energy*, 2017, **2**, 17135.
12 X. Zheng, Y. Hou, C. Bao, J. Yin, F. Yuan, Z. Huang, K. Song, J. Liu, J. Troughton, N. Gasparini, C. Zhou, Y. Lin, D.-J. Xue, B. Chen, A. K. Johnston, N. Wei, M. N. Hedhili, M. Wei, A. Y. Alsalloum, P. Maity, B. Turedi, C. Yang, D. Baran, T. D. Anthopoulos, Y. Han, Z.-H. Lu, O. F. Mohammed, F. Gao, E. H. Sargent and O. M. Bakr, Managing grains and interfaces via ligand anchoring enables 22.3%-efficiency inverted perovskite solar cells, *Nat. Energy*, 2020, **5**, 131–140.
13 D. Yu, F. Cao, J. Liao, B. Wang, C. Su and G. Xing, Direct observation of photoinduced carrier blocking in

mixed-dimensional 2D/3D perovskites and the origin, *Nat. Commun.*, 2022, **13**, 6229.
14 C. M. Wolff, L. Canil, C. Rehermann, N. Ngoc Linh, F. Zu, M. Ralaiarisoa, P. Caprioglio, L. Fiedler, M. Stolterfoht, S. Kogikoski, Jr., I. Bald, N. Koch, E. L. Unger, T. Dittrich, A. Abate and D. Neher, Perfluorinated Self-Assembled Monolayers Enhance the Stability and Efficiency of Inverted Perovskite Solar Cells, *ACS Nano*, 2020, **14**, 1445–1456.
15 Q. Wang, X. Zheng, Y. Deng, J. Zhao, Z. Chen and J. Huang, Stabilizing the α-Phase of $CsPbI_3$ Perovskite by Sulfobetaine Zwitterions in One-Step Spin-Coating Films, *Joule*, 2017, **1**, 371–382.
16 W. Xiang, Z. Wang, D. J. Kubicki, W. Tress, J. Luo, D. Prochowicz, S. Akin, L. Emsley, J. Zhou, G. Dietler, M. Grätzel and A. Hagfeldt, Europium-Doped $CsPbI_2Br$ for Stable and Highly Efficient Inorganic Perovskite Solar Cells, *Joule*, 2019, **3**, 205–214.
17 M. Saliba, T. Matsui, K. Domanski, J. Y. Seo, A. Ummadisingu, S. M. Zakeeruddin, J. P. Correa-Baena, W. R. Tress, A. Abate, A. Hagfeldt and M. Gratzel, Incorporation of rubidium cations into perovskite solar cells improves photovoltaic performance, *Science*, 2016, **354**, 206–209.
18 M. Saliba, T. Matsui, J. Y. Seo, K. Domanski, J. P. Correa-Baena, M. K. Nazeeruddin, S. M. Zakeeruddin, W. Tress, A. Abate, A. Hagfeldt and M. Gratzel, Cesium-containing triple cation perovskite solar cells: improved stability, reproducibility and high efficiency, *Energy Environ. Sci.*, 2016, **9**, 1989–1997.
19 M. Saliba, Polyelemental, Multicomponent Perovskite Semiconductor Libraries through Combinatorial Screening, *Adv. Energy Mater.*, 2019, **9**, 1803754.
20 X. Zheng, B. Chen, J. Dai, Y. Fang, Y. Bai, Y. Lin, H. Wei, X. C. Zeng and J. Huang, Defect passivation in hybrid perovskite solar cells using quaternary ammonium halide anions and cations, *Nat. Energy*, 2017, **2**, 17102.
21 R. Wang, J. Xue, K. L. Wang, Z. K. Wang, Y. Luo, D. Fenning, G. Xu, S. Nuryyeva, T. Huang, Y. Zhao, J. L. Yang, J. Zhu, M. Wang, S. Tan, I. Yavuz, K. N. Houk and Y. Yang, Constructive molecular configurations for surface-defect passivation of perovskite photovoltaics, *Science*, 2019, **366**, 1509–1513.
22 L. Fu, H. Li, L. Wang, R. Yin, B. Li and L. Yin, Defect passivation strategies in perovskites for an enhanced photovoltaic performance, *Energy Environ. Sci.*, 2020, **13**, 4017–4056.
23 E. H. Jung, N. J. Jeon, E. Y. Park, C. S. Moon, T. J. Shin, T. Y. Yang, J. H. Noh and J. Seo, Efficient, stable and scalable perovskite solar cells using poly(3-hexylthiophene), *Nature*, 2019, **567**, 511–515.
24 W. Zhou, Z. Wen and P. Gao, Less is More: Dopant-Free Hole Transporting Materials for High-Efficiency Perovskite Solar Cells, *Adv. Energy Mater.*, 2018, **8**, 1702512.
25 Q. Jiang, X. Zhang and J. You, SnO2: A Wonderful Electron Transport Layer for Perovskite Solar Cells, *Small*, 2018, **14**, 1801154.
26 L. Shi, M. P. Bucknall, T. L. Young, M. Zhang, L. Hu, J. Bing, D. S. Lee, J. Kim, T. Wu, N. Takamure, D. R. McKenzie, S. Huang, M. A. Green and A. W. Y. Ho-Baillie, Gas chromatography-mass spectrometry analyses of encapsulated stable perovskite solar cells, *Science*, 2020, **368**, 1328.
27 K. O. Brinkmann, J. Zhao, N. Pourdavoud, T. Becker, T. Hu, S. Olthof, K. Meerholz, L. Hoffmann, T. Gahlmann, R. Heiderhoff, M. F. Oszajca, N. A. Luechinger, D. Rogalla, Y. Chen, B. Cheng and T. Riedl, Suppressed decomposition of organometal halide perovskites by impermeable electron-extraction layers in inverted solar cells, *Nat. Commun.*, 2017, **8**, 13938.
28 D. Koushik, W. J. H. Verhees, Y. Kuang, S. Veenstra, D. Zhang, M. A. Verheijen, M. Creatore and R. E. I. Schropp, High-efficiency humidity-stable planar perovskite solar cells based on atomic layer architecture, *Energy Environ. Sci.*, 2017, **10**, 91–100.
29 J. Hu, L. Yan and W. You, Two-Dimensional Organic-Inorganic Hybrid Perovskites: A New Platform for Optoelectronic Applications, *Adv. Mater.*, 2018, **30**, 1802041.
30 J. V. Passarelli, D. J. Fairfield, N. A. Sather, M. P. Hendricks, H. Sai, C. L. Stern and S. I. Stupp, Enhanced Out-of-Plane Conductivity and Photovoltaic Performance in $n = 1$ Layered Perovskites through Organic Cation Design, *J. Am. Chem. Soc.*, 2018, **140**, 7313–7323.
31 L. N. Quan, M. Yuan, R. Comin, O. Voznyy, E. M. Beauregard, S. Hoogland, A. Buin, A. R. Kirmani, K. Zhao, A. Amassian, D. H. Kim and E. H. Sargent, Ligand-Stabilized Reduced-Dimensionality Perovskites, *J. Am. Chem. Soc.*, 2016, **138**, 2649–2655.
32 S. Chen, N. Shen, L. Zhang, W. Kong, L. Zhang, C. Cheng and B. Xu, Binary organic spacer-based quasi-two-dimensional perovskites with preferable vertical orientation and efficient charge transport for high-performance planar solar cells, *J. Mater. Chem. A*, 2019, **7**, 9542–9549.
33 C. M. M. Soe, W. Nie, C. C. Stoumpos, H. Tsai, J. C. Blancon, F. Liu, J. Even, T. J. Marks, A. D. Mohite and M. G. Kanatzidis, Understanding Film Formation Morphology and Orientation in High Member 2D Ruddlesden-Popper Perovskites for High-Efficiency Solar Cells, *Adv. Energy Mater.*, 2018, **8**, 1700979.
34 T. Oku, Y. Ohishi and N. Ueoka, Highly (100)-oriented $CH_3NH_3PbI_3Cl$ perovskite solar cells prepared with NH_4Cl using an air blow method, *RSC Adv.*, 2018, **8**, 10389–10395.
35 X. Zhang, G. Wu, W. Fu, M. Qin, W. Yang, J. Yan, Z. Zhang, X. Lu and H. Chen, Orientation Regulation of Phenylethylammonium Cation Based 2D Perovskite Solar Cell with Efficiency Higher Than 11%, *Adv. Energy Mater.*, 2018, **8**, 1702498.
36 W. Fu, J. Wang, L. Zuo, K. Gao, F. Liu, D. S. Ginger and A. K. Y. Jen, Two-Dimensional Perovskite Solar Cells with 14.1% Power Conversion Efficiency and 0.68% External Radiative Efficiency, *ACS Energy Lett.*, 2018, **3**, 2086–2093.
37 Z. Liu, D. Liu, H. Chen, L. Ji, H. Zheng, Y. Gu, F. Wang, Z. Chen and S. Li, Enhanced Crystallinity of Triple-Cation

Perovskite Film via Doping NH_4SCN, *Nanoscale Res. Lett.*, 2019, **14**, 304.

38 S. Thawarkar, S. R. Rondiya, N. Y. Dzade, N. Khupse and S. Jadkar, Experimental and Theoretical Investigation of the Structural and Opto-electronic Properties of Fe-Doped Lead-Free $Cs_2AgBiCl_6$ Double Perovskite, *Chem. – Eur. J.*, 2021, **27**, 7408–7417.

39 Y. Liu, H. Zhou, Y. Ni, J. Guo, R. Lu, C. Li and X. Guo, Revealing stability origin of Dion-Jacobson 2D perovskites with different-rigidity organic cations, *Joule*, 2023, **7**, 1016–1032.

40 Y. Li, J. V. Milic, A. Ummadisingu, J. Y. Seo, J. H. Im, H. S. Kim, Y. Liu, M. I. Dar, S. M. Zakeeruddin, P. Wang, A. Hagfeldt and M. Grätzel, Bifunctional Organic Spacers for Formamidinium-Based Hybrid Dion-Jacobson Two-Dimensional Perovskite Solar Cells, *Nano Lett.*, 2019, **19**, 150–157.

41 C. Liu, Z. Fang, J. Sun, M. Shang, K. Zheng, W. Yang and Z. Ge, Donor-acceptor-donor type organic spacer for regulating the quantum wells of Dion-Jacobson 2D perovskites, *Nano Energy*, 2022, **93**, 106800.

42 S. Shao, X. Cui and Z. Li, Recent Progress in Understanding the Structural, Optoelectronic, and Photophysical Properties of Lead Based Dion-Jacobson Perovskites as Well as Their Application in Solar Cells, *ACS Materials Lett.*, 2022, **4**, 891–917.

43 J. Qing, X.-K. Liu, M. Li, F. Liu, Z. Yuan, E. Tiukalova, Z. Yan, M. Duchamp, S. Chen, Y. Wang, S. Bai, J.-M. Liu, H. J. Snaith, C.-S. Lee, T. C. Sum and F. Gao, Aligned and Graded Type-II Ruddlesden-Popper Perovskite Films for Efficient Solar Cells, *Adv. Energy Mater.*, 2018, **8**, 1800185.

44 Y. Zhang, P. Wang, M. C. Tang, D. Barrit, W. Ke, J. Liu, T. Luo, Y. Liu, T. Niu, D. M. Smilgies, Z. Yang, Z. Liu, S. Jin, M. G. Kanatzidis, A. Amassian, S. F. Liu and K. Zhao, Dynamical Transformation of Two-Dimensional Perovskites with Alternating Cations in the Interlayer Space for High-Performance Photovoltaics, *J. Am. Chem. Soc.*, 2019, **141**, 2684–2694.

45 J. Gong, M. Hao, Y. Zhang, M. Liu and Y. Zhou, Layered 2D Halide Perovskites beyond the Ruddlesden-Popper Phase: Tailored Interlayer Chemistries for High-Performance Solar Cells, *Angew. Chem., Int. Ed.*, 2022, **61**, e202112022.

46 Z. Lu, X. Xu, Y. Gao, Z. Wu, A. Li, Z. Zhan, Y. Qu, Y. Cai, X. Huang, J. Huang, Z. Zhang, T. Luo, L. Peng, P. Liu, T. Shi and W. Xie, The effect of spacer cations on optoelectronic properties of two-dimensional perovskite based on first-principles calculations, *Sur. Interfaces*, 2022, **34**, 102343.

47 X. Li, J. M. Hoffman and M. G. Kanatzidis, The 2D halide perovskite rulebook: How the spacer influences everything from the structure to optoelectronic device efficiency, *Chem. Rev.*, 2021, **142**, 2230–2291.

48 J. Hu, X. Wen and D. Li, Optical properties of two-dimensional perovskites, *Front. Phys.*, 2023, **18**, 33602.

49 F. O. Saouma, C. C. Stoumpos, J. Wong, M. G. Kanatzidis and J. I. Jang, Selective enhancement of optical nonlinearity in two-dimensional organic-inorganic lead iodide perovskites, *Nat. Commun.*, 2017, **8**, 742.

50 L. Iagher and L. Etgar, Effect of Cs on the Stability and Photovoltaic Performance of 2D/3D Perovskite-Based Solar Cells, *ACS Energy Lett.*, 2018, **3**, 366–372.

51 S. Jeong, S. Seo, H. Yang, H. Park, S. Shin, H. Ahn, D. Lee, J. H. Park, N. G. Park and H. Shin, Cyclohexylammonium-Based 2D/3D Perovskite Heterojunction with Funnel-Like Energy Band Alignment for Efficient Solar Cells (23.91%), *Adv. Energy Mater.*, 2021, **11**, 2102236.

52 A. Krishna, M. A. Akhavan Kazemi, M. Sliwa, G. N. M. Reddy, L. Delevoye, O. Lafon, A. Felten, M. T. Do, S. Gottis and F. Sauvage, Defect Passivation via the Incorporation of Tetrapropylammonium Cation Leading to Stability Enhancement in Lead Halide Perovskite, *Adv. Funct. Mater.*, 2020, **30**, 1909737.

53 D. H. Cao, C. C. Stoumpos, O. K. Farha, J. T. Hupp and M. G. Kanatzidis, 2D Homologous Perovskites as Light-Absorbing Materials for Solar Cell Applications, *J. Am. Chem. Soc.*, 2015, **137**, 7843–7850.

54 Y. Fan, H. Chen, X. Liu, M. Ren, Y. Liang, Y. Wang, Y. Miao, Y. Chen and Y. Zhao, Myth behind Metastable and Stable *n*-Hexylammonium Bromide-Based Low-Dimensional Perovskites, *J. Am. Chem. Soc.*, 2023, **145**, 8209–8217.

55 H. Zheng, H. Xu, F. Zheng, G. Liu, X. Xu, S. Xu, L. Zhang and X. Pan, The Effect of Constituent Ratios and Varisized Ammonium Salts on the Performance of Two-Dimensional Perovskite Materials, *ChemSusChem*, 2020, **13**, 252–259.

56 I. Spanopoulos, I. Hadar, W. Ke, Q. Tu, M. Chen, H. Tsai, Y. He, G. Shekhawat, V. P. Dravid, M. R. Wasielewski, A. D. Mohite, C. C. Stoumpos and M. G. Kanatzidis, Uniaxial Expansion of the 2D Ruddlesden-Popper Perovskite Family for Improved Environmental Stability, *J. Am. Chem. Soc.*, 2019, **141**, 5518–5534.

57 F. Li, Y. Xie, Y. Hu, M. Long, Y. Zhang, J. Xu, M. Qin, X. Lu and M. Liu, Effects of Alkyl Chain Length on Crystal Growth and Oxidation Process of Two-Dimensional Tin Halide Perovskites, *ACS Energy Lett.*, 2020, **5**, 1422–1429.

58 J. Yan, W. Fu, X. Zhang, J. Chen, W. Yang, W. Qiu, G. Wu, F. Liu, P. Heremans and H. Chen, Highly oriented two-dimensional formamidinium lead iodide perovskites with a small bandgap of 1.51 eV, *Mater. Chem. Front.*, 2018, **2**, 121–128.

59 X. Zhang, X. Ren, B. Liu, R. Munir, X. Zhu, D. Yang, J. Li, Y. Liu, D.-M. Smilgies, R. Li, Z. Yang, T. Niu, X. Wang, A. Amassian, K. Zhao and S. Liu, Stable high efficiency two-dimensional perovskite solar cells via cesium doping, *Energy Environ. Sci.*, 2017, **10**, 2095–2102.

60 F. Han, W. Yang, H. Li and L. Zhu, Stable High-Efficiency Two-Dimensional Perovskite Solar Cells Via Bromine Incorporation, *Nanoscale Res. Lett.*, 2020, **15**, 194.

61 X. Zhang, G. Wu, S. Yang, W. Fu, Z. Zhang, C. Chen, W. Liu, J. Yan, W. Yang and H. Chen, Vertically Oriented 2D Layered Perovskite Solar Cells with Enhanced Efficiency and Good Stability, *Small*, 2017, **13**, 1700611.

62 H. Zheng, D. Liu, Y. Wang, Y. Yang, H. Li, T. Zhang, H. Chen, L. Ji, Z. Chen and S. Li, Synergistic effect of

additives on 2D perovskite film towards efficient and stable solar cell, *Chem. Eng. J.*, 2020, **389**, 124266.

63 J. Sun, N. Chandrasekaran, C. Liu, A. D. Scully, W. Yin, C. K. Ng and J. J. Jasieniak, Enhancement of 3D/2D Perovskite Solar Cells Using an F4TCNQ Molecular Additive, *ACS Appl. Energy Mater.*, 2020, **3**, 8205–8215.

64 B. Chen, Z. Liu, K. Meng, Z. Qiao, Y. Zhai, R. Yu, L. Wu, M. Xiao, L. Pan, L. Zheng and G. Chen, In Situ Observing and Tuning the Crystal Orientation of Two-Dimensional Layered Perovskite via the Chlorine Additive, *Nano Lett.*, 2022, **22**, 7826–7833.

65 T. Duong, H. Pham, Y. Yin, J. Peng, M. A. Mahmud, Y. Wu, H. Shen, J. Zheng, T. Tran-Phu, T. Lu, L. Li, A. Kumar, G. G. Andersson, A. Ho-Baillie, Y. Liu, T. White, K. Weber and K. Catchpole, Efficient and stable wide bandgap perovskite solar cells through surface passivation with long alkyl chain organic cations, *J. Mater. Chem. A*, 2021, **9**, 18454–18465.

66 B. Chen, H. Chen, Y. Hou, J. Xu, S. Teale, K. Bertens, H. Chen, A. Proppe, Q. Zhou, D. Yu, K. Xu, M. Vafaie, Y. Liu, Y. Dong, E. H. Jung, C. Zheng, T. Zhu, Z. Ning and E. H. Sargent, Passivation of the Buried Interface via Preferential Crystallization of 2D Perovskite on Metal Oxide Transport Layers, *Adv. Mater.*, 2021, **33**, 2103394.

67 G. Yang, Z. Ren, K. Liu, M. Qin, W. Deng, H. Zhang, H. Wang, J. Liang, F. Ye, Q. Liang, H. Yin, Y. Chen, Y. Zhuang, S. Li, B. Gao, J. Wang, T. Shi, X. Wang, X. Lu, H. Wu, J. Hou, D. Lei, S. K. So, Y. Yang, G. Fang and G. Li, Stable and low-photovoltage-loss perovskite solar cells by multifunctional passivation, *Nat. Photonics*, 2021, **15**, 681–689.

68 H. Wang, J. Ma and D. Li, Two-Dimensional Hybrid Perovskite-Based van der Waals Heterostructures, *J. Phys. Chem. Lett.*, 2021, **12**, 8178–8187.

69 H. Wang, Y. Chen and D. Li, Two/Quasi-two-dimensional perovskite-based heterostructures: construction, properties and applications, *Int. J. Extrem. Manuf.*, 2023, **5**, 012004.

70 N. Zhou, Y. Shen, L. Li, S. Tan, N. Liu, G. Zheng, Q. Chen and H. Zhou, Exploration of Crystallization Kinetics in Quasi Two-Dimensional Perovskite and High Performance Solar Cells, *J. Am. Chem. Soc.*, 2018, **140**, 459–465.

71 H. Tsai, R. Asadpour, J. C. Blancon, C. C. Stoumpos, J. Even, P. M. Ajayan, M. G. Kanatzidis, M. A. Alam, A. D. Mohite and W. Nie, Design principles for electronic charge transport in solution-processed vertically stacked 2D perovskite quantum wells, *Nat. Commun.*, 2018, **9**, 2130.

72 I. C. Smith, E. T. Hoke, D. Solis-Ibarra, M. D. McGehee and H. I. Karunadasa, A layered hybrid perovskite solar-cell absorber with enhanced moisture stability, *Angew. Chem., Int. Ed.*, 2014, **53**, 11232–11235.

73 J. Qing, S. Ramesh, Q. Xu, X. K. Liu, H. Wang, Z. Yuan, Z. Chen, L. Hou, T. C. Sum and F. Gao, Spacer Cation Alloying in Ruddlesden-Popper Perovskites for Efficient Red Light-Emitting Diodes with Precisely Tunable Wavelengths, *Adv. Mater.*, 2021, **33**, 2104381.

74 D. Lin, X. Xu, T. Zhang, N. Pang, J. Wang, H. Li, T. Shi, K. Chen, Y. Zhou, X. Wang, J. Xu, P. Liu and W. Xie, The selection strategy of ammonium-group organic salts in vapor deposited perovskites: From dimension regulation to passivation, *Nano Energy*, 2021, **84**, 105893.

75 S. Song, S. J. Yang, J. Choi, S. G. Han, K. Park, H. Lee, J. Min, S. Ryu and K. Cho, Surface Stabilization of a Formamidinium Perovskite Solar Cell Using Quaternary Ammonium Salt, *ACS Appl. Mater. Interfaces*, 2021, **13**, 37052–37062.

76 Q. Li, Y. Dong, G. Lv, T. Liu, D. Lu, N. Zheng, X. Dong, Z. Xu, Z. Xie and Y. Liu, Fluorinated Aromatic Formamidinium Spacers Boost Efficiency of Layered Ruddlesden-Popper Perovskite Solar Cells, *ACS Energy Lett.*, 2021, **6**, 2072–2080.

77 S. Cui, J. Wang, H. Xie, Y. Zhao, Z. Li, S. Luo, L. Ke, Y. Gao, K. Meng, L. Ding and Y. Yuan, Rubidium Ions Enhanced Crystallinity for Ruddlesden-Popper Perovskites, *Adv. Sci.*, 2020, **7**, 2002445.

78 H. Yu, Y. Xie, J. Zhang, J. Duan, X. Chen, Y. Liang, K. Wang and L. Xu, Thermal and Humidity Stability of Mixed Spacer Cations 2D Perovskite Solar Cells, *Adv. Sci.*, 2021, **8**, 2004510.

79 S. Ramos-Terrón, A. D. Jodlowski, C. Verdugo-Escamilla, L. Camacho and G. de Miguel, Relaxing the Goldschmidt Tolerance Factor: Sizable Incorporation of the Guanidinium Cation into a Two-Dimensional Ruddlesden-Popper Perovskite, *Chem. Mater.*, 2020, **32**, 4024–4037.

80 X. Yan, S. Hu, Y. Zhang, H. Li and C. Sheng, Methylammonium acetate as an additive to improve performance and eliminate *J–V* hysteresis in 2D homologous organic-inorganic perovskite solar cells, *Sol. Energy Mater. Sol. C*, 2019, **191**, 283–289.

81 S. Yu, Y. Yan, Y. Chen, P. Chábera, K. Zheng and Z. Liang, Enabling room-temperature processed highly efficient and stable 2D Ruddlesden-Popper perovskite solar cells with eliminated hysteresis by synergistic exploitation of additives and solvents, *J. Mater. Chem. A*, 2019, **7**, 2015–2021.

82 Z. Li, B. Ma, Y. Xu, Y. Lei, W. Lan, G. Wang, W. Li, Q. Wang, H. L. Zhang and Z. Jin, N-methyl-2-pyrrolidone Iodide as Functional Precursor Additive for Record Efficiency 2D Ruddlesden-Popper $PEA_2Cs_{n-1}Pb_nI_{3n+1}$ Solar Cells, *Adv. Funct. Mater.*, 2021, **31**, 2106380.

83 H. Zheng, T. Zhang, Y. Wang, C. Li, Z. Su, Z. Wang, H. Chen, S. Yuan, Y. Gu, L. Ji, J. Li and S. Li, Zwitterion-Assisted Crystal Growth of 2D Perovskites with Unfavorable Phase Suppression for High-Performance Solar Cells, *ACS Appl. Mater. Interfaces*, 2022, **14**, 814–825.

84 F. S. Ghoreishi, V. Ahmadi, R. Poursalehi, M. SamadPour, M. B. Johansson, G. Boschloo and E. M. J. Johansson, Enhanced performance of $CH_3NH_3PbI_3$ perovskite solar cells via interface modification using phenyl ammonium iodide derivatives, *J. Power Sources*, 2020, **473**, 228492.

85 X. Zhu, S. Zuo, Z. Yang, J. Feng, Z. Wang, X. Zhang, S. Priya, S. F. Liu and D. Yang, In Situ Grain Boundary Modification via Two-Dimensional Nanoplates to Remarkably Improve

Stability and Efficiency of Perovskite Solar Cells, *ACS Appl. Mater. Interfaces*, 2018, **10**, 39802–39808.

86 R. He, Z. Yi, Y. Luo, J. Luo, Q. Wei, H. Lai, H. Huang, B. Zou, G. Cui, W. Wang, C. Xiao, S. Ren, C. Chen, C. Wang, G. Xing, F. Fu and D. Zhao, Pure 2D Perovskite Formation by Interfacial Engineering Yields a High Open-Circuit Voltage beyond 1.28 V for 1.77-eV Wide-Bandgap Perovskite Solar Cells, *Adv. Sci.*, 2022, **9**, e2203210.

87 B. Liu, J. Hu, D. He, L. Bai, Q. Zhou, W. Wang, C. Xu, Q. Song, D. Lee, P. Zhao, F. Hao, X. Niu, Z. Zang and J. Chen, Simultaneous Passivation of Bulk and Interface Defects with Gradient 2D/3D Heterojunction Engineering for Efficient and Stable Perovskite Solar Cells, *ACS Appl. Mater. Interfaces*, 2022, **14**, 21079–21088.

88 R. L. Milot, R. J. Sutton, G. E. Eperon, A. A. Haghighirad, J. Martinez Hardigree, L. Miranda, H. J. Snaith, M. B. Johnston and L. M. Herz, Charge-Carrier Dynamics in 2D Hybrid Metal-Halide Perovskites, *Nano Lett.*, 2016, **16**, 7001–7007.

89 Q. Cheng, B. Wang, G. Huang, Y. Li, X. Li, J. Chen, S. Yue, K. Li, H. Zhang, Y. Zhang and H. Zhou, Impact of Strain Relaxation on 2D Ruddlesden-Popper Perovskite Solar Cells, *Angew. Chem., Int. Ed.*, 2022, **61**, e202208264.

90 T. Liu, Y. Jiang, M. Qin, J. Liu, L. Sun, F. Qin, L. Hu, S. Xiong, X. Jiang, F. Jiang, P. Peng, S. Jin, X. Lu and Y. Zhou, Tailoring vertical phase distribution of quasi-two-dimensional perovskite films via surface modification of hole-transporting layer, *Nat. Commun.*, 2019, **10**, 878.

91 C. Liang, K. M. M. Salim, P. Li, Z. Wang, T. M. Koh, H. Gu, B. Wu, J. Xia, Z. Zhang, K. Wang, T. Liu, Q. Wei, S. Wang, Y. Tang, G. Shao, Y. Song, N. Mathews and G. Xing, Controlling the film structure by regulating 2D Ruddlesden-Popper perovskite formation enthalpy for efficient and stable tri-cation perovskite solar cells, *J. Mater. Chem. A*, 2020, **8**, 5874–5881.

92 S. Zhao, J. Xie, G. Cheng, Y. Xiang, H. Zhu, W. Guo, H. Wang, M. Qin, X. Lu, J. Qu, J. Wang, J. Xu and K. Yan, General Nondestructive Passivation by 4-Fluoroaniline for Perovskite Solar Cells with Improved Performance and Stability, *Small*, 2018, **14**, e1803350.

93 J. Hu, I. W. H. Oswald, S. J. Stuard, M. M. Nahid, N. Zhou, O. F. Williams, Z. Guo, L. Yan, H. Hu, Z. Chen, X. Xiao, Y. Lin, Z. Yang, J. Huang, A. M. Moran, H. Ade, J. R. Neilson and W. You, Synthetic control over orientational degeneracy of spacer cations enhances solar cell efficiency in two-dimensional perovskites, *Nat. Commun.*, 2019, **10**, 1276.

94 J. Shi, Y. Gao, X. Gao, Y. Zhang, J. Zhang, X. Jing and M. Shao, Fluorinated Low-Dimensional Ruddlesden-Popper Perovskite Solar Cells with over 17% Power Conversion Efficiency and Improved Stability, *Adv. Mater.*, 2019, **31**, 1901673.

95 S. Paek, C. Roldan-Carmona, K. T. Cho, M. Franckevicius, H. Kim, H. Kanda, N. Drigo, K. H. Lin, M. Pei, R. Gegevicius, H. J. Yun, H. Yang, P. A. Schouwink, C. Corminboeuf, A. M. Asiri and M. K. Nazeeruddin, Molecular Design and Operational Stability: Toward Stable 3D/2D Perovskite Interlayers, *Adv. Sci.*, 2020, **7**, 2001014.

96 X. Li, W. Hu, Y. Shang, X. Yu, X. Wang, W. Zhou, M. Wang, Q. Luo, C.-Q. Ma, Y. Lu and S. Yang, Phenylformamidinium-enabled quasi-2D Ruddlesden-Popper perovskite solar cells with improved stability, *J. Energy Chem.*, 2022, **66**, 680–688.

97 G. Liu, X.-X. Xu, S. Xu, L. Zhang, H. Xu, L. Zhu, X. Zhang, H. Zheng and X. Pan, Passivation effect of halogenated benzylammonium as a second spacer cation for improved photovoltaic performance of quasi-2D perovskite solar cells, *J. Mater. Chem. A*, 2020, **8**, 5900–5906.

98 G. Liu, H. Zheng, X. Xu, S. Xu, X. Zhang, X. Pan and S. Dai, Introduction of Hydrophobic Ammonium Salts with Halogen Functional Groups for High-Efficiency and Stable 2D/3D Perovskite Solar Cells, *Adv. Funct. Mater.*, 2019, **29**, 1807565.

99 Z. Wang, Q. Wei, X. Liu, L. Liu, X. Tang, J. Guo, S. Ren, G. Xing, D. Zhao and Y. Zheng, Spacer Cation Tuning Enables Vertically Oriented and Graded Quasi-2D Perovskites for Efficient Solar Cells, *Adv. Funct. Mater.*, 2020, **31**, 2008404.

100 X. Fu, T. He, S. Zhang, X. Lei, Y. Jiang, D. Wang, P. Sun, D. Zhao, H.-Y. Hsu, X. Li, M. Wang and M. Yuan, Halogen-halogen bonds enable improved long-term operational stability of mixed-halide perovskite photovoltaics, *Chem*, 2021, **7**, 3131–3143.

101 L. Wang, Q. Zhou, Z. Zhang, W. Li, X. Wang, Q. Tian, X. Yu, T. Sun, J. Wu, B. Zhang and P. Gao, A guide to use fluorinated aromatic bulky cations for stable and high-performance 2D/3D perovskite solar cells: The more fluorination the better?, *J. Energy Chem.*, 2022, **64**, 179–189.

102 G. Liu, H. Zheng, H. Xu, L. Zhang, X. Xu, S. Xu and X. Pan, Interface passivation treatment by halogenated low-dimensional perovskites for high-performance and stable perovskite photovoltaics, *Nano Energy*, 2020, **73**, 104753.

103 W. Wang, Z. Su, B. Sun, L. Tao, H. Gu, W. Hui, Q. Wei, W. Shi, X. Gao, Y. Xia and Y. Chen, Toward Efficient and Stable Perovskite Solar Cells by 2D Interface Energy Band Alignment, *Adv. Mater. Interfaces*, 2020, **8**, 2001683.

104 X. Li, W. Ke, B. Traore, P. Guo, I. Hadar, M. Kepenekian, J. Even, C. Katan, C. C. Stoumpos, R. D. Schaller and M. G. Kanatzidis, Two-Dimensional Dion-Jacobson Hybrid Lead Iodide Perovskites with Aromatic Diammonium Cations, *J. Am. Chem. Soc.*, 2019, **141**, 12880–12890.

105 H. Lai, D. Lu, Z. Xu, N. Zheng, Z. Xie and Y. Liu, Organic-Salt-Assisted Crystal Growth and Orientation of Quasi-2D Ruddlesden-Popper Perovskites for Solar Cells with Efficiency over 19, *Adv. Mater.*, 2020, **32**, e2001470.

106 Y. Yan, S. Yu, A. Honarfar, T. Pullerits, K. Zheng and Z. Liang, Benefiting from Spontaneously Generated 2D/3D Bulk-Heterojunctions in Ruddlesden-Popper Perovskite by Incorporation of S-Bearing Spacer Cation, *Adv. Sci.*, 2019, **6**, 1900548.

107 Y. Dong, D. Lu, Z. Xu, H. Lai and Y. Liu, 2-Thiopheneformamidinium-Based 2D Ruddlesden-Popper Perovskite Solar Cells with Efficiency of 16.72% and Negligible Hysteresis, *Adv. Energy Mater.*, 2020, **10**, 2000694.

108 U. Gunes, E. Bag Celik, C. C. Akgul, M. Koc, M. Ameri, B. E. Uzuner, M. Ghasemi, M. C. Sahiner, İ. Yildiz, H. Z. Kaya, S. Yerci and G. Gunbas, A Thienothiophene-Based Cation Treatment Allows Semitransparent Perovskite Solar Cells with Improved Efficiency and Stability, *Adv. Funct. Mater.*, 2021, **31**, 2103130.

109 J. Wang, Z. Zhang, J. Liang, Y. Zheng, X. Wu, C. Tian, Y. Huang, Z. Zhou, Y. Yang, A. Sun, Z. Chen and C. C. Chen, Bottom-Up Templated and Oriented Crystallization for Inverted Triple-Cation Perovskite Solar Cells with Stabilized Nickel-Oxide Interface, *Small*, 2022, **18**, e2203886.

110 G. Liu, H. Zheng, J. Ye, S. Xu, L. Zhang, H. Xu, Z. Liang, X. Chen and X. Pan, Mixed-Phase Low-Dimensional Perovskite-Assisted Interfacial Lead Directional Management for Stable Perovskite Solar Cells with Efficiency over 24%, *ACS Energy Lett.*, 2021, **6**, 4395–4404.

111 A. A. Sutanto, N. Drigo, V. I. E. Queloz, I. Garcia-Benito, A. R. Kirmani, L. J. Richter, P. A. Schouwink, K. T. Cho, S. Paek, M. K. Nazeeruddin and G. Grancini, Dynamical evolution of the 2D/3D interface: a hidden driver behind perovskite solar cell instability, *J. Mater. Chem. A*, 2020, **8**, 2343–2348.

112 M. Salado, M. Andresini, P. Huang, M. T. Khan, F. Ciriaco, S. Kazim and S. Ahmad, Interface Engineering by Thiazolium Iodide Passivation Towards Reduced Thermal Diffusion and Performance Improvement in Perovskite Solar Cells, *Adv. Funct. Mater.*, 2020, **30**, 1910561.

113 J. Qiu, Y. Lin, X. Ran, Q. Wei, X. Gao, Y. Xia, P. Müller-Buschbaum and Y. Chen, Efficient and stable Ruddlesden-Popper layered tin-based perovskite solar cells enabled by ionic liquid-bulky spacers, *Sci. China: Chem.*, 2021, **64**, 1577–1585.

114 H. Zheng, W. Wu, H. Xu, F. Zheng, G. Liu, X. Pan and Q. Chen, Self-Additive Low-Dimensional Ruddlesden-Popper Perovskite by the Incorporation of Glycine Hydrochloride for High-Performance and Stable Solar Cells, *Adv. Funct. Mater.*, 2020, **30**, 2000034.

115 C. Ma and N.-G. Park, Paradoxical Approach with a Hydrophilic Passivation Layer for Moisture-Stable, 23% Efficient Perovskite Solar Cells, *ACS Energy Lett.*, 2020, **5**, 3268–3275.

116 T. Liu, J. Guo, D. Lu, Z. Xu, Q. Fu, N. Zheng, Z. Xie, X. Wan, X. Zhang, Y. Liu and Y. Chen, Spacer Engineering Using Aromatic Formamidinium in 2D/3D Hybrid Perovskites for Highly Efficient Solar Cells, *ACS Nano*, 2021, **15**, 7811–7820.

117 R. Garai, R. K. Gupta, M. Hossain and P. K. Iyer, Surface recrystallized stable 2D-3D graded perovskite solar cells for efficiency beyond 21%, *J. Mater. Chem. A*, 2021, **9**, 26069–26076.